AD-A190 508 FILM COOLING EFFECTIVENESS ON A FLAT PLATE IN HIGH FREE-STREAM TURBULENCE (U) AIR FORCE INST OF TECH WRIGHT-PATTERSON AFB OH SCHOOL OF ENGI G W JUMPER

1/1

UNCLASSIFIED DEC 87 AFIT/GAE/AA/87D-7 F/G 20/13 NL

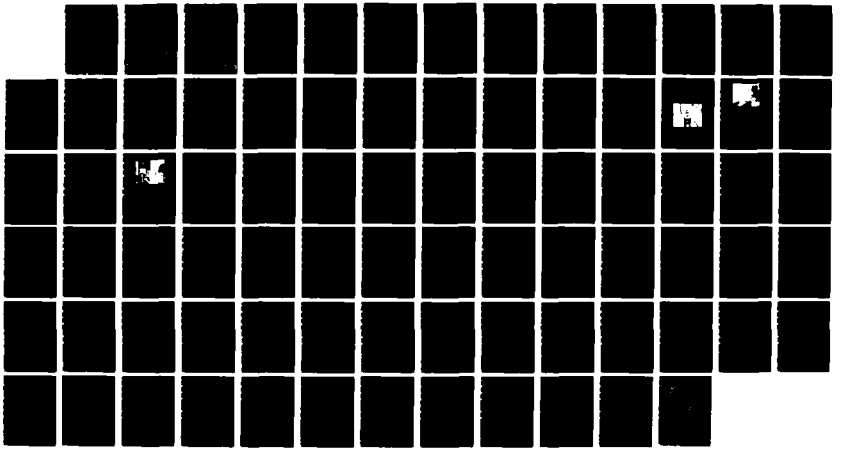

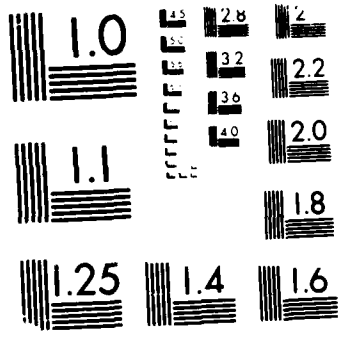

MICROCOPY RESOLUTION TEST CHART

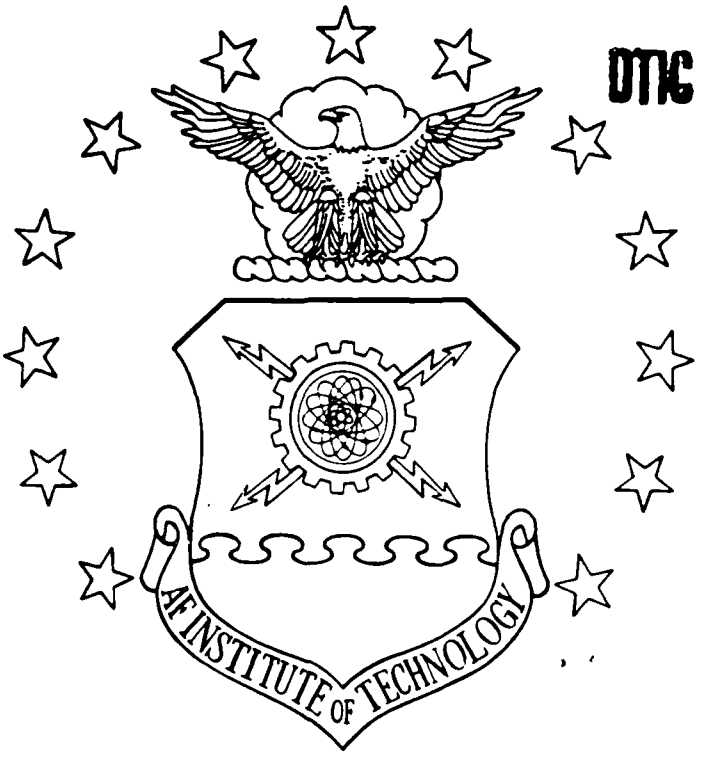

FILM COOLING EFFECTIVENESS ON A FLAT PLATE IN HIGH FREE-STREAM TURBULENCE USING A SINGLE ROW OF 30° SLANT-HOLE INJECTORS

THESIS

AFIT/GAE/AA/87D-7 GEOFFREY W. JUMPER
Major, USAF

DEPARTMENT OF THE AIR FORCE
AIR UNIVERSITY
AIR FORCE INSTITUTE OF TECHNOLOGY

Wright-Patterson Air Force Base, Ohio

AFIT/GAE/AA/87D-7

FILM COOLING EFFECTIVENESS ON A FLAT PLATE IN HIGH FREE-STREAM TURBULENCE USING A SINGLE ROW OF 30° SLANT-HOLE INJECTORS

THESIS

AFIT/GAE/AA/87D-7 GEOFFREY W. JUMPER
Major, USAF

Approved for public release; distribution unlimited

AFIT/GAE/AA/87D-7

FILM COOLING EFFECTIVENESS ON A FLAT PLATE IN HIGH FREE-STREAM TURBULENCE USING A SINGLE ROW OF 30° SLANT-HOLE INJECTORS

THESIS

Presented to the Faculty of the School of Engineering

of the Air Force Institute of Technolgy

Air University

in Partial Fulfillment of the

Requirements for the Degree of

Master of Science in Aeronautical Engineering

Geoffrey W. Jumper, B.S., M.S.

Major, USAF

December 1987

Preface

Heat transfer and cooling in gas turbines is one of the crucial fields in the quest for higher performance of jet engines. To meet the needs for tomorrows aircraft, the thermodynamic efficiency of the engines must improve. One approach is to increase the turbine inlet gas temperature. Higher temperature gases passing over the turbine blades may result in a large heat flux to the surface unless some method of blade protection, such as film cooling, is used. There is a lack of understanding on film cooling and to compensate manufacturers have been overcooling critical components.

In this thesis, I collected data on film cooling effectiveness on a flat plate in high free-stream turbulence using a single row of 30° slant-hole injectors. A wall jet was used to provide the high turbulence. The major objective of the study is to examine the effect of high turbulence on film cooling effectiveness.

I wish to express my graditude to my thesis advisor, Dr. William C. Elrod for his guidance and to Dr. James E. Hitchcock for stimulating an interest in heat transfer in the third of the Jumper boys to have taken courses under him. This study would not have been possible without the countless hours of help from my thesis sponsor, Dr. Richard B. Rivir, whose guidance was critical throughout the project. Finally, my wife, Sevim, deserves special thanks for her understanding and support.

Computer: Apple Macintosh 128, HP 9845C
Software: MacWrite 4.5, HP Basic
Printer: Imagewriter I, HP 9872A Plotter

Geoffrey W. Jumper

Table of Contents

List of Figures

List of Figures (Cont.)

List of Tables

List of Symbols

English Letter Symbols

A	Area (ft^2)
D	Inside diameter of ASME nozzle, 8 in.
f	Coefficient of friction
FST	Free-stream turbulence
fps	Velocity, (ft/sec)
h	Heat transfer coefficient (W/ft^2-F)
k	Thermal conductivity (B/hr-ft-F)
k_t	Eddy conductivity (B/hr-ft-F)
M	Blowing rate, ($\rho_f U_f / \rho_\infty U_\infty$), also refered to RHO-VELOCITY or RHO-VELOCITY RATIO in graphs
Nu	Nusselt number (hD/k)
$\dot{q}''$	Heat flux per unit area (W/ft^2)
Re	Reynolds number ($\rho U_\infty X/\mu$)
St	Stanton number ($h/\rho U_\infty Cp$)
T	Mean temperature (R, F)

List of Symbols (cont.)

Tu	Free-Stream Turbulence Intensity
U	Total velocity component in X dirtection (fps)
USL	Unheated starting length, 5 ft section of flat plate
U_{max}	Maximum U along the y axis
X	Distance down the plate from the 8 inch ASME nozzle used for Re's and distance from injectors for station numbers
X'	Distance down the plate from the 8 inch ASME used for development of the cooling model
y	Vertical distance from the plate (ft)
Y_{max}	Distance above the plate where U is a maximum (ft)

Greek Letters

η	Film Cooling Effectiveness defined in Figure 1
μ	Dynamic Viscosity (lb_m/ft-sec)
ρ	Density (lb_m/ft^3)
δ	Boundary layer thickness (inches)

List of Symbols (cont.)

Subscripts

a	Ambient conditions outside of wall jet
aw	Adiabatic wall condition, evaluated at the plate
f	Evaluated film cooling temperature, T_f
sl	Sub-layer used in the Film Cooling Model
∞	Evaluated at free-stream state outside of sensor boundary layer, usually at Y_{max}
*	Without Blowing, No Film Cooling

ABSTRACT

In the continuing search to understand the mechanisms influencing film cooling effectiveness, this thesis examines film cooling effectiveness on a flat plate in high free-stream turbulence using a single row of 30° slant-hole injectors. The primary area of focus is the area within 42 diameters down-stream of injection. Of interest are blowing rates for optimum film cooling effectivenss within 10 diameters down-stream of injection, and the decay of film cooling effectiveness down the plate. Free-stream velocities from 50 - 175 fps and free-stream turbulence intensities from 13.5 - 18.5% were examined. Changes in Reynolds number or free-stream turbulence had little effect on blowing rates for optimum film cooling effectiveness. In comparison with tests conducted in low free-stream turbulence, around 5%, higher free-stream turbulence causes a faster decay in film cooling effectiveness down the plate.

FILM COOLING EFFECTIVENESS ON A FLAT PLATE IN HIGH FREE-STREAM TURBULENCE USING A SINGLE ROW OF 30° SLANT-HOLE INJECTORS

I. Introduction

Background

Turbine blade cooling in gas turbines is one of the crucial fields in the quest for higher performance of jet engines. To meet the needs for tomorrows aircraft, the thermodynamic efficiency of the engine must improve. One approach to improve the thermodynamic efficiency is to increase the turbine inlet gas temperature. Higher temperature gases passing over the turbine blades result in a large heat flux to the surface unless some method of blade protection is used. One method is film cooling which injects a coolant through the surface of the turbine blade, into the boundary layer, to provide a heat sink for the hot gases and protect the surface. The coolant is air taken from the compressor section of the engine. Air removed from the compressor is air which will produce no work for the engine and reduces efficiency.

How much coolant is required? There is lack of understanding on this subject and to compensate manufactures have been overcooling critical components. The need for study in this area has been recognized and some data has been collected. Past reasearch, conducted in wind tunnels at low turbulence intensities, around 5 to 7%, observed significant relationships between film cooling effectiveness and blowing rates. Work done by Goldstein (1), using a single circular injector normal to the flow, noted several interesting results. As the blowing of the coolant begins, there is an initial bathing of of the plate which provides a layer of protection from the free-stream. As the blowing rate and the mass injected in the boundry layer increases towards an optimum, the effectiveness also increases. Physically, there is a thickening of the protective bathing layer. At blowing rates at or below optimum, the injected flow remains close to the wall. A further increase in the blowing rate increases the penetration of the jet into the main flow which increases mixing and decreases cooling effectiveness (1:258). Goldstein found blowing rates between 0.4 -0.5 resulted in optimum film cooling effectiveness, within 10 diameters of injection. Past 10 diameters down-stream of injection, film cooling effectiveness

decays. Thus film cooling effectiveness is a mzximum within 10 diameters. In another study, Goldstein found, for a 35° slant hole injector, the optimum mixture ratios were between 0 .5 - 0.6 (2:385,3:599). The reason of the increase in optimum blowing rate is the inclined jet has a smaller component of momentum in the direction normal to the flow, or in other words, its pointed in the right direction.

Most of Goldstein's work was done at low free-stream velocities around 50 fps. Results from work done by J. C. Han at higher free-stream velocities of 168 fps and turbulence intensities around 5% also noted optimum film cooling effectiveness at blowing rates between 0.5 -0.6 within 10 diameters of injection (4:5,5:38). A significant limitation of past studies is they were performed with relatively low levels of turbulence intensity. The flow in turbines is highly complex and turbulence intensities are considered to be much higher, perhaps in the 15-20% range. Therefore, other methods must be considered to learn more about film cooling in a highly turbulent flow.

The wall jet provides high levels of free-stream turbulence similiar to those in a jet engine turbine. Suggested readings to better understand the nature of the wall jets can be found in Adrian Bejan's text

on Convective Heat Transfer (6:283-295) and a more in depth analysis and literature review can be found in a Doctorial by MacArthur (7).

Care must also be taken when comparing data using a wall jet with that from a wind tunnel. Where wind tunnels provide a steady free-stream velocity, the wall jet has a pear shaped velocity profile which rapidly decays. It is difficult to take data in this environment. In this study, data was taken for a set station velocity. When obtaining data at stations down the plate, the wall jet nozzle velocity was increased along with the secondary flow to maintain desired blowing rates. Thus several parameters were changed. To compare free-stream velocity and temperature with that from a wind tunnel, a reference point had to be selected. The wall jet velocity distribution acquires the nature of boundry layer near the wall but becomes a free jet further away. The boundry layer edge is defined using a technique in Schlichting's text Boundary-Layer Theory. The point where the maximum velocity of the jet is Umax and that height is defined as Ymax (8:751).

Objective

This study was conducted to investigate film cooling on a flat plate in high free-stream turbulence. Specific objectives were:

a) Design and construct an improved flat plate test apparatus.

b) Obtain data on blowing rates for optimum cooling effectiveness over a range of Reynolds numbers.

c) Obtain velocity and temperature profiles with blowing.

d) Obtain heat transfer data with blowing.

Experimental Approach

The primary drive of this study was to obtain data not yet available in the turbine engine industry, specifically cooling effectiveness data from a flat plate in a highly turbulent flow. To be able to compare results with other studies which were done in wind-tunnels, care was taken to insure results were calculated from basic definitions. The definitions used in this study can be found in Kays and Crawford's text Heat and Mass Transfer (9:224), and work done by Richard J. Goldstein (10,11,12). Film cooling effectiveness, η , as defined in Heat and Mass Transfer, is used in the present study. Given in Figure 1, the adiabatic surface temperature, T_{aw}, the free-stream temperature, T_{∞}, and the cooling-fluid temperature, T_f, are used to define film cooling effectiveness.

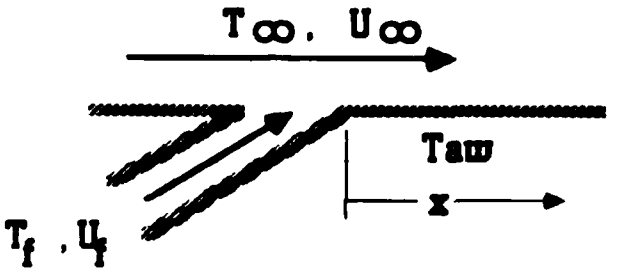

$$\Pi = \frac{Taw - T\infty}{T_f - T\infty}$$

Π = Film Cooling Effectiveness

Figure 1: Film Cooling Effectiveness Defination.

Past studies of film cooling effectiveness found that η is primarily a function of a blowing rate parameter M and the distance down-stream of injection. The blowing rate parameter used in this and other studies is defined as $M = (\rho_f U_f) / (\rho_\infty U_\infty)$.

The adiabatic wall temperature was used for the surface temperature and the static temperature of the flow was used as the coolant flow temperature (1:255, 13:190-192). Mass flows were determined by using isentropic relationships and experimentally determined coefficients of discharge for both the main and secondary flows (14:73-100, 20). Primary flow velocity measurements were made

using either a single hot-wire or hot-film anemometer. All velocity readings were compared against a pitot-probe for accuracy. Oil contamination of the air supply proved to be a big problem resulting in considerable "down-time" due to loss of a hot wire, re-calibration, and retesting. The hot-film anemometer proved to be more reliable, although it too was prone to errors caused by oil contamination. A 5 ft unheated starting length was used which included a 30° slant hole injection system.

For heat transfer tests, the flat plate test section was powered by a.c. power. The uniform plate heat flux could be determined from known resistence/ current/ and voltage. The local heat transfer coefficients could then be determined by methods developed by Han (15) and procedures by MacMullin (16).

II. Experimental Apparatus

The test section consisted of an instrumented flat plate, unheated starting length with seven 30° slant-hole injectors (only five injectors were used), traversing system, 8 in. diameter ASME nozzle and air supply system. Tests were conducted in a 40 ft by 80 ft laboratory area with a ceiling approximately 23 ft high. Air flowed out of the area through two adjustable 6 ft by 14 ft metal sliding doors. Data was taken in an adjacent control room with reinforced glass observation windows.

Driscol Flat Plate Test Section

The "Driscol" table is named after one of the designers and builders of the table who has been fighting an unfortunately losing battle against cancer. The table consisted of a 2 ft by 10 ft constant heat flux section, and a 2 ft by 5 ft unheated starting section. The heat flux is generated by electric resistant heating in 3 parallel stripes of 6 inch wide by 0.002 inch thick stainless steel foil (302 stainless, full hard, tension leveled, 2% flat, 0.002 in. thick) mounted on an insulated substrate. For accurate and repeatable data, several problems had to be overcome in the design of the table.

The first problem was to prevent heat conduction through the plate.

The solution from past experiments was a 1/16 in. fiberglass laminate surface, insulated on the bottom by 4 in. of urethane foam (k=0.025 Btu/hr-ft-F), reinforced on the bottom and sides with wood, and covered with a layer of fiberglass. The entire plate rests on a wood frame support. The 5 ft. unheated starting section was constructed of a smooth composite wood surface and housed the injection system for film cooling. Two 5.5 in high by 180 in. long wall boards were used on the sides in an attempt to maintain, as much as possible, a 2-D flow down the plate. The wall boards are considered not to have an effect on the center foil where the data was taken.

The second and most difficult problem was with the instrumentation. The goal was to measure "fairly quickly" the temperature changes down the surface of the plate. The options were for the desired response were limited to thin thermocouple wires. Thicker wires would require a longer time to stabilize at a given test condition and would also increase conduction down the wires and through the table. For the "quicker" response time, 6 arrays of 0.005 in. iron-constantan bead-welded thermocouples were used. In the film cooling effectiveness study, only the first 4 arrays were used in data taking. Each array was

welded to the underside of the center 6 in. wide stainless steel foil and threaded through small holes in the urethane and support structure. The thin iron-constantan wire gave the quicker response time and limited conduction through the table, but proved to be very fragil. The bead-welded thermocouples were very easy to break and required considerable care during construction. The thermocouple wires were then connected to two Celesco 150° F reference junctions located under the plate.

The third problem was the thermal expansion of the steel foil when used to provide the constant heat flux. When heated, it expanded and created wrinkles causing problems in the boundry layer. Another problem was the foil had been glued to the table and the heat caused "out gasing" of the glue to produced air bubbbles under the foil. The solution for this problem was to covered the length of the table with 6 in. wide stainless steel foil in 3 parallel rows connected in series by copper bus bars. At the end of the table, the bus bars were connected to 30 pound weights pulling the foil tight over a set of rollers. When the foil expanded, the weights pulled on the foil and kept the surface flat. To prevent the foil from lifting off the table during tests, rows of double-sided 0.001 in.

tape were used between the foil and the table. Figure 2 shows the roller-weight system to keep the foil tight and Figure 3 shows the lay-out of the table top with injectors and traversing system. Figure 4 shows the table top dimensions, note only the first 4 thermocouple stations used in the film cooling effectiveness test are shown.

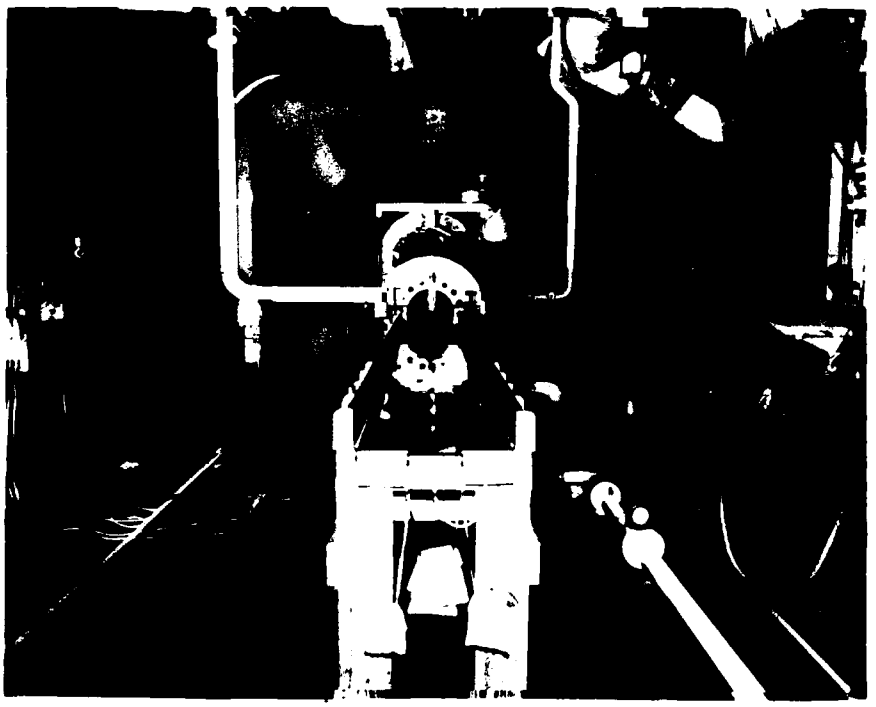

Figure 2 Roller Weight System

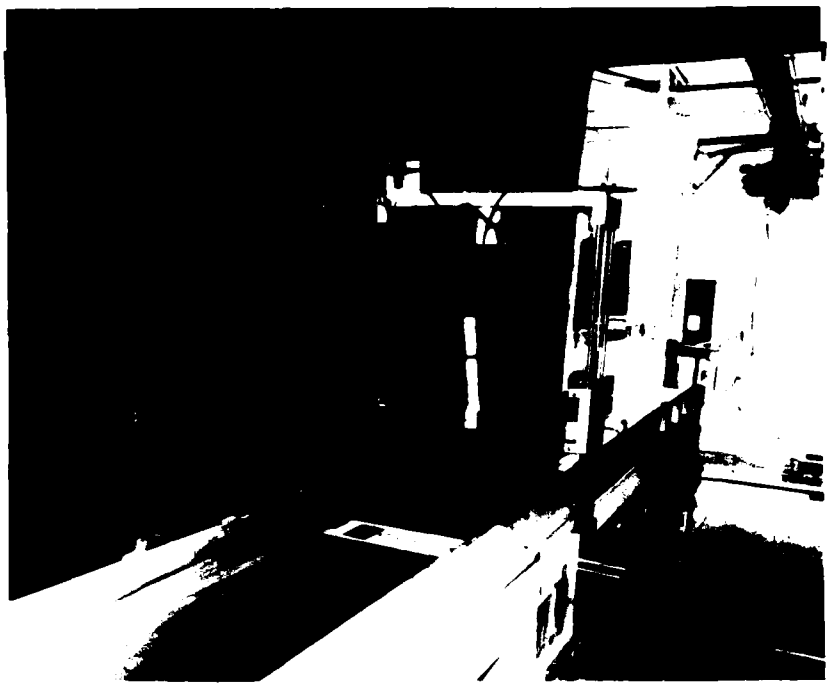

Figure 3 Table Layout

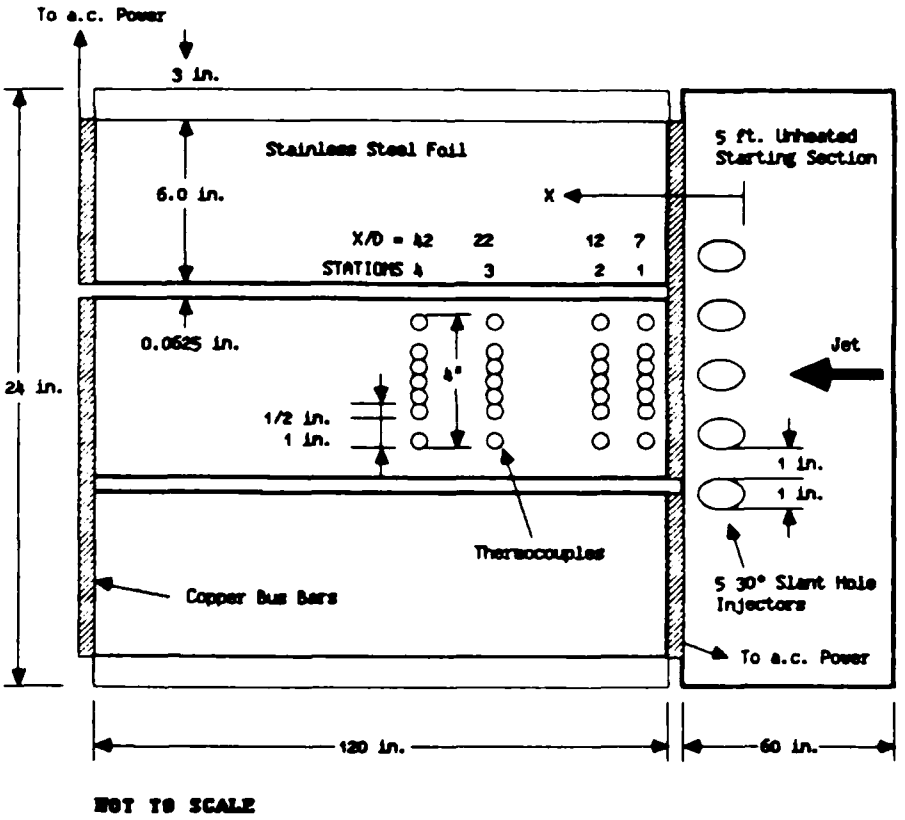

Figure 4 Table Top Dimensions

"The metal foil was powered by 240 volts a.c. through a Superior Electric 7.8 kVa powerstat (variac) and twin Topaz 4.3 kVa isolation transformers. The energy dissipation was calculated by measurement of the RMS voltage drop across the plate simultaneously with the voltage across a calibrated General Electric (GE) 0.002 ohm shunt in series with the foil. RMS voltage measurements were made with Hewlett-Packard (HP) 3497A digital multimeters (16:8).

Traversing System

The traversing system was developed in past experiments (16:9). It provided a means of accurately positioning the velocity and temperature sensors vertically above the plate surface. The centerline position was manually adjusted along a set of fine threaded rods. "The sensor platform was adjusted vertically by twin precision stainless steel threaded rods which were rotated by a Superior Electric Slo-Syn synchronous M093-FC07 stepping motor through a chain and sprocket assembly. The stepping motor was controlled by a Slo-Syn ST101 translator and Trygon Electronics HR 20-1.5 power supply. The stepping motor was activated either by a three-position (up, down, off) switch and/or by the data acquisition software program. Maximum travel speed in the vertical

direction was approximately 0.25 ft/min and reversal hysteresis was 0.01 in. An Astrosystems encoder transducer was mounted on one of the drive sprockets and transmitted position information to a digital decoder in the control room. Position error of the apparatus for a single direction traverse was less than 0.001 in." (16:9-12)

Air Supply

The main air supply was provide by Ingersol-Rand compressors rated at 300 psia and 2.5 lbm/sec. Depending on the velocity required for each experiement, 2 or 3 compressors were used. The idea was to keep the compressors "completely loaded" at all times to provide a steady air flow. The air was settled in a 32 in. diameter by 60 in. long chamber. Tank conditions were constantly monitored with a 24-gauge iron-constantan thermocouple and a precision micromanometer. Temperatures varied from 78 to 85° F depending on environmental conditions. The wall jet was produced by an 8 in. diameter circular ASME nozzle with a contraction ratio of 16:1 and an assumed coefficient of discharge of 1. Exit velocities ranged from 100 to 300 fps.

The secondary or cooling air supply was produced by a A/M 32C-4 aircraft ground air conditioner unit. The unit is capable of supplying air

at a constant temperature in the range from 20 to 100° F. Prior to injection, the coolant was stilled in 2x2x2 ft stilling chamber where conditions were also constantly monitored. Tank temperatures were varied from 56 to 98° F depending on the particular experiment. To determine the mass flow rate from the secondary air supply, the coefficient of discharge was determined to be 0.61. The methods for determining the coefficient of discharge were those found in the ASME text Fluid Meters, Their Theory and Applications(20). The mass air flow rates for both chambers were manually controlled by gate valves and calculated by isentropic relationships and the experimentally measured coefficients of discharge (14:73-100, 20). Figure 5 shows the secondary air supply system. Note the flexible rubber/cotton weave hose in Figure 5. The flexible hose is a safety feature designed to rupture at 40 psi before the possibility of the secondary stilling tank failing. The secondary stilling tank is square, reducing it's ability to withstand pressure, and it was possible to choke the flow in the injectors and cause the pressure to increase to the point of failure. The flexible hose was designed to fail before the stilling tank.

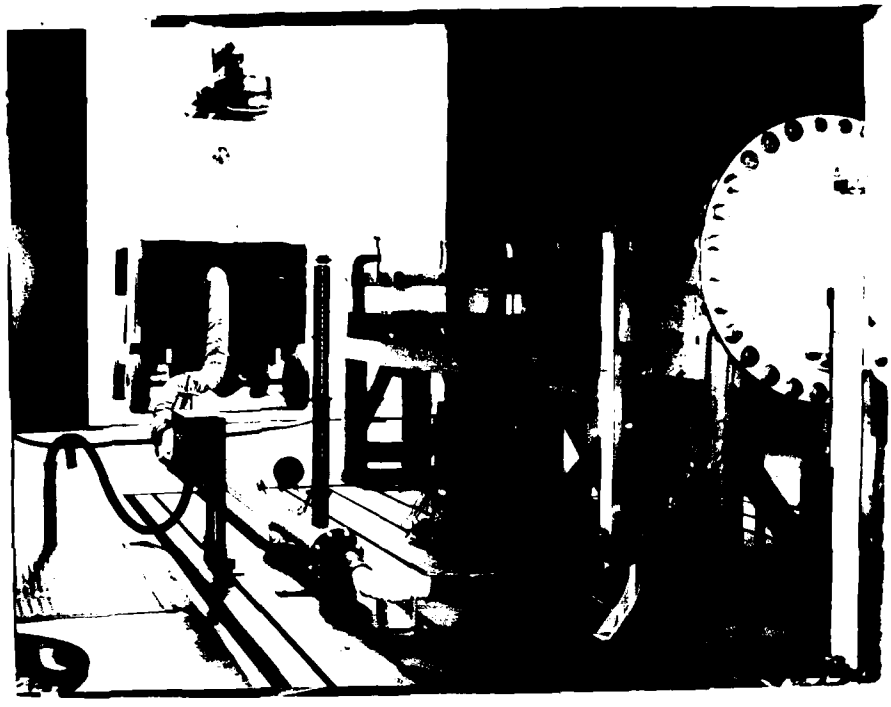

Figure 5 Secondary Air System

Data Acquisition

The heart of the data acquisition system is a HP 9845C computer. The computer uses the HP-IB interface bus to relay all software directed data acquisition. All thermocouple and anemometer voltages were measured by an 80 channel HP 3497A Data Acquisition Controller Unit and Digital Voltmeter at a maximum rate of 25 channels/sec. Velocity measures were obtained from a single hot-wire or hot-film sensor

controlled by a Thermo-Systems, Inc. (TSI) IFA-100 constant temperature anemometer. A discussion of constant temperature hot-wire anemometers is contained in Hinze's classic text, "Turbulence" (17:41). The same data acquisition and data reduction techniques used in MacMullin's report were used in this investigation (16:25). The anemometer output was paralleled to the HP 3497A for scanning mean voltage and to an HP 3478A multimeter for RMS Voltage measurements. Standard 1210-T-1.5 hot-wire and 1220-20 hot-film anemometer senors were used and velocities obtained were compared against data obtained using a United Sensor total pressure KBA-8 miniature sensing Kiel probe. Boundary layer temperature measurements where made with a United Sensor thermal boundary layer probe (Model-BT-.020-12-C-11-.650-2) with a 0.02 in. diameter sensing head.

III. Experimental Procedures and Data Reduction

Overall Tests Performed

Four types of tests where performed during this study:

a) Validation of the new table.

b) Film cooling effectiveness.

c) Velocity/temperature profiles.

d) Heat transfer.

Raw data was collected from 46 thermocouples, mean and RMS bridge voltages from a constant temperature anemometer, 2 kiel probe pressures, a large and small chamber pressure differential, plate and shunt RMS voltages, sensor position readout and ambient pressure. For the film cooling effectiveness tests, velocity/temperature profile tests, and heat transfer tests, data was obtained at specific locations on the flat plate. The stations are refered to in terms of diameters down-stream of the secondary flow injectors. For example station 1 was at X/D = 7 or 7 injector diameters down-stream of the secondary air flow injection. The Reynolds numbers are based on distance down the flat plate from the 8" circular ASME nozzle and the free-stream velocity and

fluid properties. The high free-stream turbulence intensity is a result of the ASME nozzle refered to in literature as a wall jet. A wa ' has the characteristic of producing high free-stream turbulence an .c amount of turbulence intensity is a direct result of the ASME nozzle exit velocity. Increasing the nozzle exit velocity increased the free-stream turbulence. Distance down the plate also increased the free-stream turbulence intensity. By setting a desired station velocity established the turbulence intensity

Validation Test

Since this a continuation of a long term study and major changes had been done to the apparatus, it was important to validate results from the new table by comparing them against past results. The unheated starting section was used without film cooling. Heat transfer data was taken using the same techniques and procedures developed by MacMullin (16:16-19). Details of this test are not provided since this was a check on the table and not development of new data. The results were comparable with past studies and thus validating the table.

Film Cooling Effectiveness Tests

Film cooling effectiveness tests were done for the adiabatic case. No heat was applied to the plate. The plate was only used to measure temperatures down-stream of film cooling injection. In this case, the free-stream temperature was normally around 78°F and the film cooling temperature was about 20°F lower. The temperature gradient was decreasing from the free-stream to the cooling flow and adiabatic surface temperature was measured on the table. Free-stream velocity/temperature data was taken at the point where the free-stream velocity was a maximum. The data was taken over a range of station free-stream velocities (50 - 175 fps), blowing rates (0.2 - 1.7) measured at point of injection, and station turbulence intensities (13.5 -18.5%). A kiel probe was used to measure velocities in two places:

1) The free-stream velocity was measured at the station as a check on the hot wire/film.

2) Just up-stream of the cooling injectors to calculate the blowing rate. Care was taken not to seperate or blow the boundary layer off the table with the cooling flow. This set a limit on the highest blowing rate at low free-steam velocities (50 fps). At the higher free-stream

velocities this was not a problem, but the blowing rate was limited by the amount of cooling flow that could be pumped through the air conditioning unit. The procedure was:

a) Set the free-stream velocity at the station and monitor conditions.

b) Set the film cooling flow and monitor conditions.

c) When conditions stabilized, measure the free-stream velocity with a kiel probe just up-stream of the cooling injectors and at the station.

All station temperatures (X/D = 7, 12, 22, and 42) where monitored and displayed on the HP 9845C computer and when all conditions were met, the data was taken. The data was immediately reduced after each test to catch errors. The next step was to set a new blowing rate by adjusting the cooling flow and holding the free-stream velocity constant. After all the blowing rate data was taken for a set free-stream velocity, the station velocity was changed and the entire test repeated.

Velocity/Temperature Profiles

The purpose of obtaining velocity and temperature profiles perpendicular to the plate was to ensure the boundary layer had not

seperated or was not blown off the table and to compare with MacMullin's results (16:54-55) and other work (18:73) being done in the area. Although this check was always taken in the cooling effectiveness tests by using a kiel probe, this test also had the purpose of providing a profile for comparision with other work done in this area. For this specific test, data was taken at station 3 where X/D = 22 or 22 diameters down-stream of the secondary air flow injectors. 22 diameters was considered far enough down-stream of the disturbance caused by mixing of the secondary and primary flows at the injectors but not too far so that the effects of injection could be measured. The procedure was:

a) The temperature probe and hot film were set to 0.1 inch from the table surface. The maximum free-stream velocity was set to 175 fps and the blowing rate was set to an optimum of 0.6. Conditions were monitored until stable. Then the maximum free-stream velocity was checked to ensure conditions had not changed. When all conditions were met, data was taken.

b) The probes were raised by 0.005 inches near the plate and 0.01 inches when the measured velocity was near U_{max}, when conditions

restabilized/checked, and data taken.

c) Step b was repeated until the probes were 4.75 inches above the plate where the free-stream velocity was rapidly decaying and well outside the area of interest. The data was then reduced and checked for errors.

Heat Transfer Tests

The purpose of these tests was to provide heat transfer data comparing the film cooling to non-film cooling case. Data for the free-stream was taken at the point were the velocity was a maximum. This data was obtained with an inverted temperature gradient from that in the turbine section of a jet engine where the gradient is from the hot gas to the cooler turbine blades. In this test, the plate was hottest, the cooling flow was next cooler, and the free-stream the coolest. Data was taken at 175 fps station velocity and at an optimum blowing rate parameter of 0.6. The procedure was:

a) Set the free-stream flow and allow conditions to stabilize while constantly monitoring conditions.

b) Set the film cooling flow and again constantly monitor conditions. For the without cooling cases, the cooling flow was

completely turned off.

c) Set the plate voltage. Monitor temperatures to ensure the entire plate was hotter than the free-stream or film cooling air yet not hot enough to damage the test stand. The limiting temperature of the plate was 130° F.

d) Monitor the environmental conditions around the room so the free-stream temperature was the same as the ceiling temperature. The reason for this was to minimize heat transfer between the room environment and the free-stream.

All the temperatures were monitored and displayed on the HP 9845C computer and when the desired test condition was established, the data was taken. The process was repeated at each station. Data reduction was done in the same manner as in MacMullin's thesis (16:19-20) and checked for errors. Errors were caused by oil contamination of the hot wire/film, a loss of a thermocouple which produced bad heat transfer data, or the free-stream conditions sometimes changed if one of the compressors changed its operating conditions. If any occured, they were corrected and tests were repeated.

IV. Film Cooling Model

Development of a model is useful to gain insight how turbulence affects film cooling effectiveness and to aid in understanding of the data obtained from this study. The actual flow is highly comlpex and difficult to model. Consider the top view of an injector as shown in Figure 6 below:

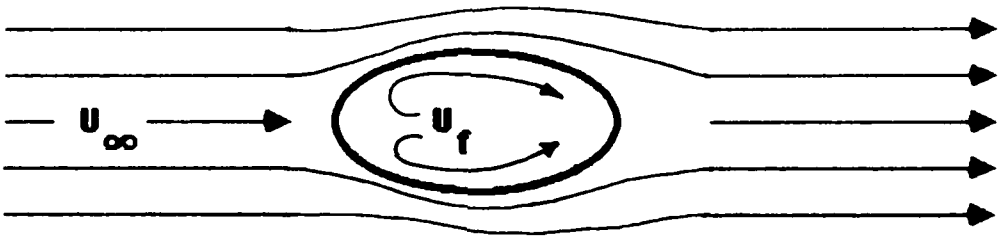

Figure 6 Top View of Injector

Mixing begins when the two flows meet at the plate surface. The free-stream flow stagnates just in front of the injected flow and then accelerates around. This produces vortices as the free-stream flow tries to carry the secondary flow along. The vortices continue to grow as the free-stream flow bends the jet parallel to the plate. The result is

a complex interaction between the two flows. A three-dimensional view given by Goldstein (2:385) is shown in Figure 7 below:

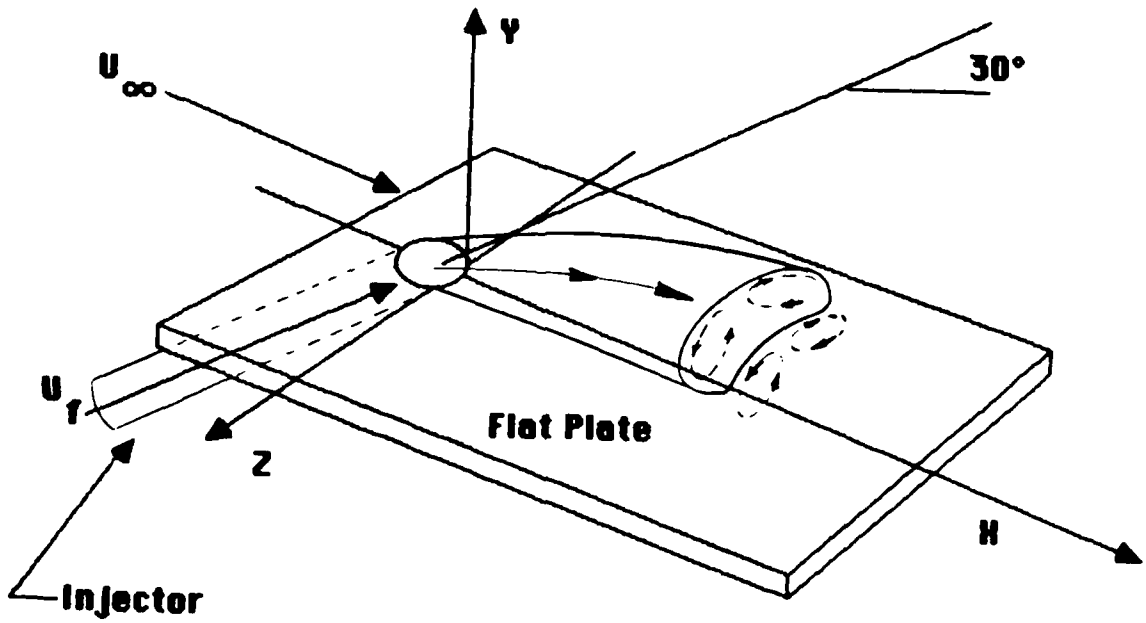

Figure 7 Three-Dimensional view of an Injector

The figure represents a blowing rate which will produce optimal film cooling effectiveness within ten diameters down-stream of injection. Modeling Figure 7 would be very difficult and fortunately it is not

necessary. To gain insight on how turbulence effects film cooling effectiveness, consider a simpler two-dimensional turbulent flow model with a two layer system as shown in Figure 8 below:

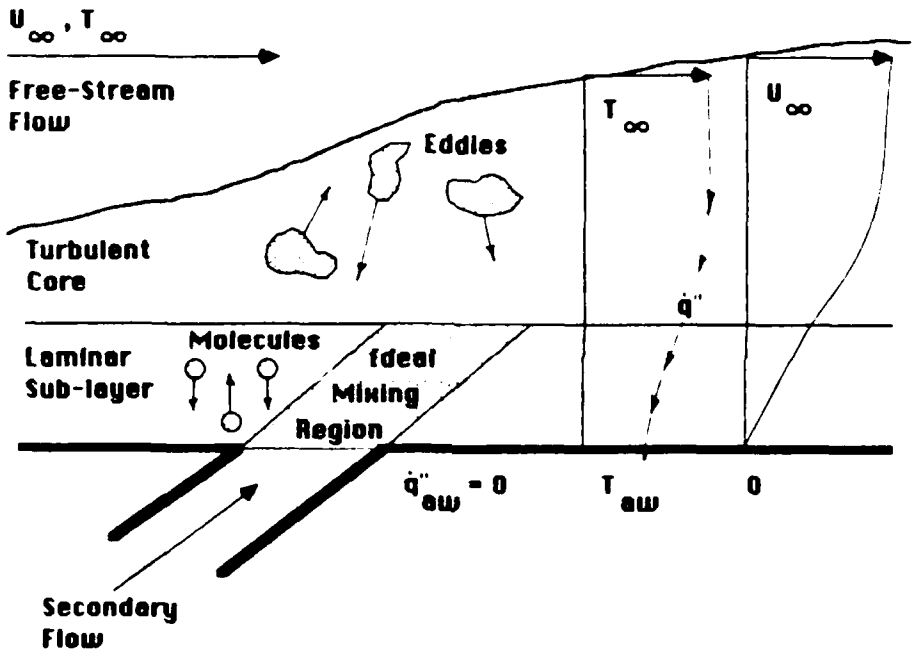

Figure 8 Two Layer Turbulent Model

The flow is divided into a laminar sub-layer and a turbulent core. In the laminar sub-layer, the mechanism for heat transfer is random collision of molecules.

The heat flux, $\dot{q}''$, is described by:

$$\dot{q}'' = -k \frac{\partial T}{\partial y}$$

In the sub-layer, the thermal conductivity, k, is a molecular conductivity. The driving force for heat transfer is the $\partial T/\partial y$ term. A thicker sub-layer will have a smaller heat flux. An ideal mixing region is pictured. The plate surface is adiabatic, $\dot{q}''_{aw} = 0$, and $\partial T/\partial y$. Continuum flow assumes the velocity of the laminar flow is zero at the surface of the plate. At the edge of the sub-layer, the velocity is approximately half of the free stream velocity. Figure 8 shows the sub-layer enlarged compared to the turbulent core, in reality the sub-layer is very thin. Where the turbulent core is about 1.6 inches thick, the sub-layer is less than 0.05 inches. The adiabatic surface temperature, T_{aw}, is shown and heat flux, $\dot{q}''$, is going towards the plate because the free-stream is hotter than the secondary flow.

In the turbulent core, the mechanism for heat transfer is movement of molecules grouped in eddies. It is convient to speak of an

eddy conductivity, k_t (9,205). The eddies vary in size and temperature and the heat transfer is now driven by $\partial T/\partial y$ and k_t:

$$\dot{q}'' = -k_t \frac{\partial T}{\partial y}$$

Since q" is proportional to a temperature difference, ΔT, an efficiency for the transfer of energy, a heat transfer coefficient, h, is defined as:

$$h = \dot{q}'' / (T_w - T_\infty)$$

In the case of film cooling:

$$h = \dot{q}'' / (T_{aw} - T_\infty)$$

What would be the effect of higher turbulence on film cooling? Consider a heat transfer solution for constant free-stream velocity and surface temperature using the two layer system in Figure 8.

A simplified solution for the Stanton number for gases is: (9:213)

$$St = \frac{.029}{Re^{0.2} \; Pr^{0.4}} \qquad (1)$$

This is a valid solution for moderate turbulence and will follow the same trend for high Reynolds numbers where the coefficient will change slightly (16:61). A relationship between higher turbulence levels, heat transfer, and film cooling can be developed. A non-dimensional y^+ is defined as:

$$y^+ = \frac{y \sqrt{\frac{gc \; \tau w}{\rho}}}{\nu}$$

Where the coefficient of friction, f, is defined by:

$$f = \frac{\tau w}{\frac{\rho U_\infty^2}{2 gc}}$$

thus:

$$y^+ = \frac{y U_\infty}{\nu} \sqrt{\frac{gc \; \tau w}{\rho \; U_\infty^2}} = \frac{y U_\infty}{\nu} \sqrt{\frac{f}{2}} \qquad (2)$$

Using the Reynolds analogy:

$$\frac{f}{2} = St\ Pr^{0.4}$$

and substituting for St from Eq (1), the coefficient of friction is:

$$\frac{f}{2} = .029 / Re^{0.2}$$

Substitute into Eq (2), and assuming $y = \delta_{sl}$ at $y^+ = 30$:

$$30 = \frac{\delta_{sl}\ U_\infty\ H'}{H'\ \nu} \sqrt{\frac{.029}{Re^{0.2}}}$$

$$\delta_{sl} = \frac{30\ H'}{\sqrt{.029}\ Re^{0.9}} \qquad (3)$$

Divide Eq (1) by Eq (3):

$$\frac{St}{\delta_{sl}} = \frac{\dfrac{.029}{Re^{0.2}\,Pr^{0.4}}}{\dfrac{30\,H'}{\sqrt{.029}\;Re^{0.9}}} = \frac{.029\sqrt{.029}}{30\,Pr^{0.4}\,(gc\mu)^{0.7}}\;\frac{\rho\,U_\infty}{H'^{0.3}}$$

Combining constant terms and defining C_0 as:

$$C_0 = \frac{.029\sqrt{.029}}{30\,Pr^{0.4}\,(gc\mu)^{0.7}}$$

and substituting gives Eq (4):

$$\frac{St}{\delta_{sl}} = \frac{C_0\,(\rho U_\infty)^{0.7}}{H'^{0.3}} \qquad (4)$$

Using the same model as in Figure 8 and adding a differential control volume, dx long and δ_{sl} high, as shown in figure 9 below:

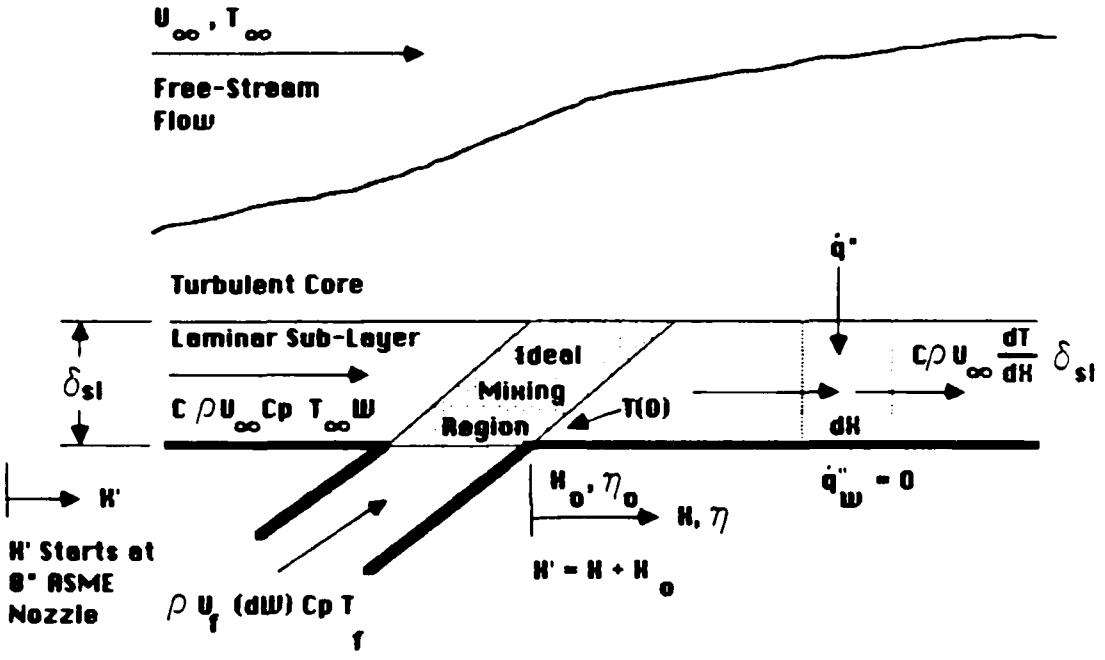

Figure 9 Two Layer Model with Control Volume

Writing a energy balance for the differential control volume:

$$C\,(\rho U_{\infty}\,Cp)\;\delta_{sl}\;W\;\frac{dT}{dX}\;dX\;-\;\dot{q}''\;W\;dX$$

Simplifing:

$$C\,(\rho\, U_{\infty} Cp)\;\delta_{sl}\,\frac{dT}{dH} = \dot{q}'' \qquad (5)$$

With $\dot{q}''$ flowing into the control volume and also noting that $T = T_{aw}$:

$$\dot{q}'' = -h\,(T - T_{\infty}) = -St\,(\rho\, U_{\infty} Cp)\,(T - T_{\infty})$$

Substituting q" into equation 5:

$$C\,(\rho\, U_{\infty}\, Cp)\;\delta_{sl}\;\frac{dT}{dH} = -St\,(\rho U_{\infty}\, Cp)\,(T - T_{\infty})$$

$$C\;\delta_{sl}\;\frac{dT}{dH} = -St\,(T - T_{\infty})$$

Using seperation of variables:

$$\frac{1}{T - T_{\infty}}\,dT = -\frac{St}{C\,\delta_{sl}}\,dH \qquad (6)$$

Integrating:

$$\int_{T(0)}^{T} \frac{1}{T - T_\infty}\, dT = \int_{H_0}^{H} - \frac{C_0 (\rho U_\infty)^{0.7}}{C H'^{0.3}}\, dH$$

$$\frac{T - T_\infty}{T(0) - T_\infty} = e^{-C' (\rho U_\infty)^{0.7} (H' - H_0^{0.7})} \tag{7}$$

$$\frac{T - T_\infty}{T(0) - T_\infty} = e^{-C^* Re^{0.7} \left(1 - \left(\frac{H_0}{H'}\right)\right)^{0.7}} \tag{8}$$

Evaluating film cooling effectiveness at x = 0:

$$\eta_o = \frac{T(0) - T_\infty}{T_f - T_\infty}$$

noting:

$$\frac{\eta}{\eta_o} = \frac{T - T_\infty}{T(0) - T_\infty} = e^{-C^* Re^{0.7} \left(1 - \left(\frac{H_0}{H'}\right)\right)^{0.7}}$$

This model allows for a few observations. If at least two data points are known, then one can solve for C* and the film cooling effectiveness at x = 0, η_o, assuming perfect mixing occurs in the mixing region. The

model also gives and indication of how fast film cooling effectiveness will decay down the plate. Recall from Eq (4), if ρU_∞ increases then the heat transfer coefficient, h, will also increase and the sub-layer thickness will decrease. This will have the effect of increasing the decay in film cooling effectiveness because the Reynolds number, Re, will increase in Eq (8). This model would indicate that increased turbulence intensity levels will decrease film cooling effectiveness down the plate. The model is summarized in Figure 10 below:

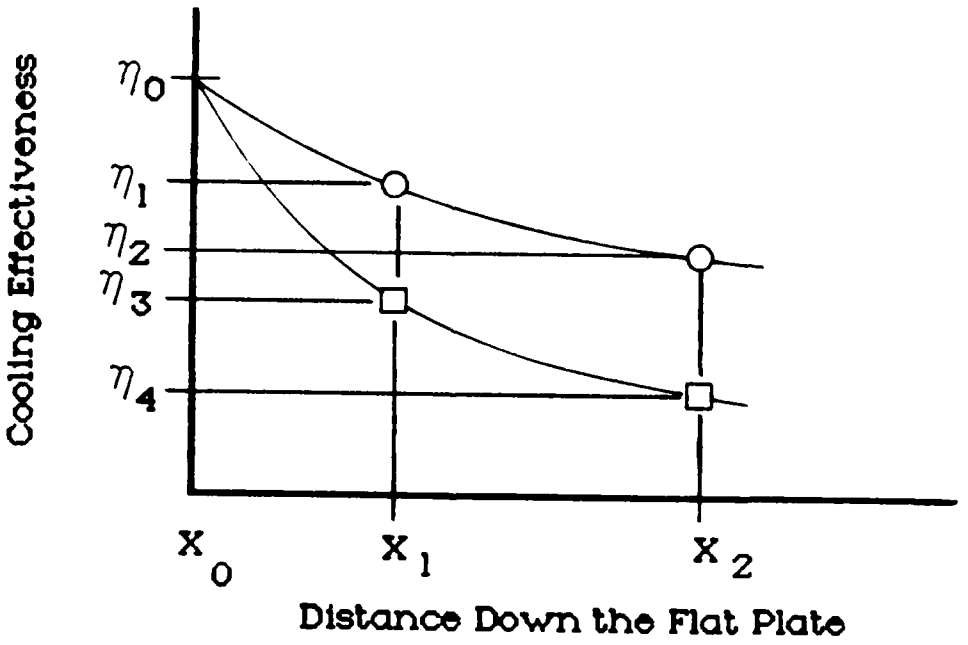

Figure 10 Model Plot

V. Results and Discussion

All the tests in this study were performed at turbulence intensities of 13.5 - 18.5%. The order of the tests and results is:

a) Cooling effectivenes.

b) Velocity/temperature profiles.

c) Heat transfer.

Cooling Effectiveness Tests

A major interest of this study is the effect of turbulence intensity on cooling effectiveness. Tests were run over a velocity range of 50 - 175 fps and turbulence intensities of 13.5 - 18.5%. Although the range of free-stream turbulence intensity is somewhat limited, the importance is the data collected is three times the free-stream turbulence intensity levels for similar work done in wind tunnels.

The effects on cooling effectiveness are effects that occur in the boundary layer. For a given free-stream turbulence, boundary layer turbulence increases with Reynolds number. Increasing free-stream turbulence, increases boundary layer turbulence for the same Reynolds number. Turbulence intensity varied in one of two ways. At a given station, the free-stream turbulence intensity was increased by increasing

the 8 inch ASME nozzle exit velocity. For a set station velocity, turbulence intensity increased down-stream on the plate. Table 1 gives the free-stream turbulence intensity for a given station velocity and station.

Table 1 Turbulence intensities on the flat plate

	Turbulence Intensity [%]			
Station Velocity [fps]	Station 1 X/D = 7	Station 2 X/D = 12	Station 3 X/D = 22	Station 4 X/D = 42
50	14.3	15.0	15.0	15.5
100	14.0	14.0	15.0	15.5
110	13.5	14.1	15.8	17.0
125	13.6	14.9	15.8	17.0
175	15.5	15.8	16.1	18.5

Results are normally discussed in terms of station velocities and Reynolds numbers, based on distance down the plate from the ASME nozzle, increased with increases in station velocity or by increased distance down the plate. Table 2 gives the Reynolds number for a given station free-stream velocity and station number.

Table 2 Reynolds numbers on the flat plate

	Reynolds Numbers [x10^{-6}]			
Station Velocity [fps]	Station 1 X/D = 7	Station 2 X/D = 12	Station 3 X/D = 22	Station 4 X/D = 42
50	1.61	2.02	2.55	2.99
100	3.25	3.45	4.23	4.95
110	3.58	3.80	4.36	5.45
125	4.00	4.29	4.90	6.13
175	6.12	6.30	7.20	8.62

Results are presented by three parameter relationships:

a) Cooling effectiveness vs. blowing rate parameter plotted for a set free-stream velocity and position down the flat plate.

b) Cooling effectiveness vs. distance down the flat plate for a set velocity and blowing rate.

c) Cooling effectiveness vs. velocity at a set station and blowing rate parameter.

Cooling Effectiveness vs. Blowing Rate Parameter:

All the data for the cooling effectiveness had a common result. At station 1, a distance of 7 diameters down stream (X/D = 7), the optimum

film cooling effectiveness was achieved with a blowing rate parameter between 0.5 and 0.6. Changes in the Reynolds number had little effect. Figure 11 groups all the free-stream velocities at station 1, X/D=7, which displays a range in Reynolds numbers representing changes in station velocity.

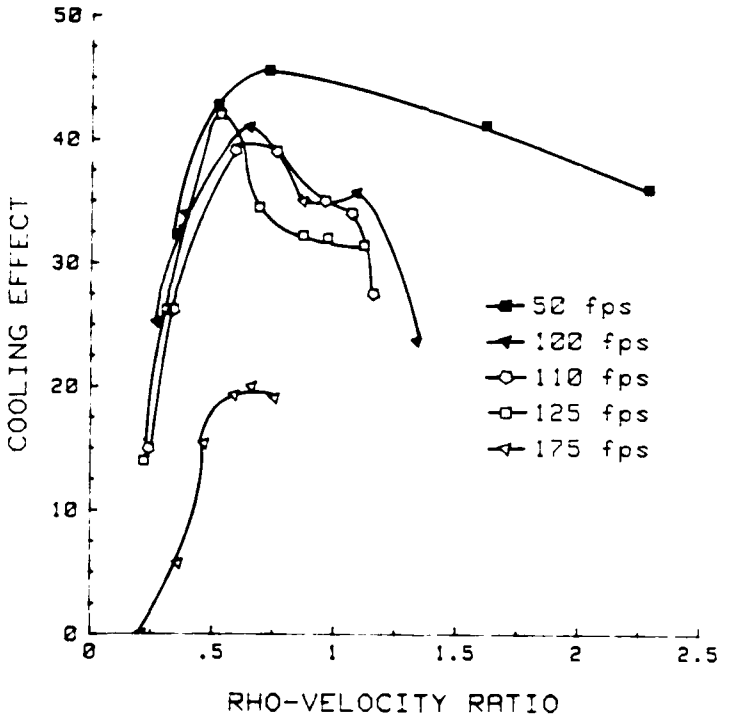

Figure 11 X/D = 7, Tu = 14.3 - 15.5%

Increased Reynolds numbers had little effect on the optimum blowing rate, but did have a strong reducing effect on the maximum cooling effectiveness. For Reynolds numbers from 1.61 - 4.00 X 10^6, cooling effectiveness reached a maximum of 40 - 45 percent, but at a Reynolds number of 6.12 X 10^6, the cooling effectiveness was only 20 percent. Approximately a 50% reduction in cooling effectiveness.

Cooling effectiveness decreases down the plate. Figure 12 represents cooling effectiveness at X/D = 12.

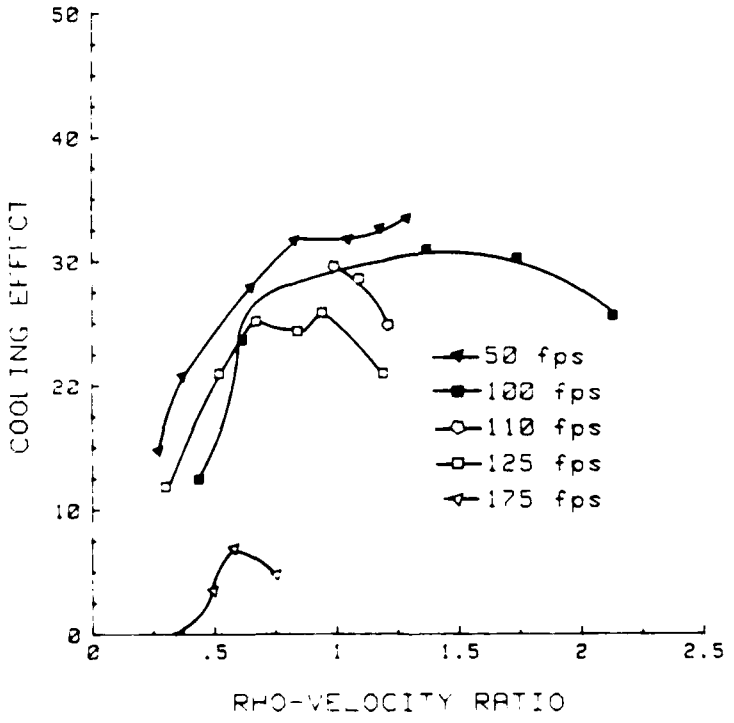

Figure 12 X/D = 12, Tu = 15.0 - 15.8%

The change in cooling effectiveness from a station velocity of 125 fps, Reynolds numbers 4.29 X 10^6, to 175 fps, Reynolds number of 6.3 X 10^6, was more than a 50% reduction. The trend is similar to X/D = 7. The slight increase in Reynolds number and free-stream turbulence intensity appears to have a large effect on cooling effectiveness. The same trend was repeated at X/D = 22 which is displayed in Figure 13.

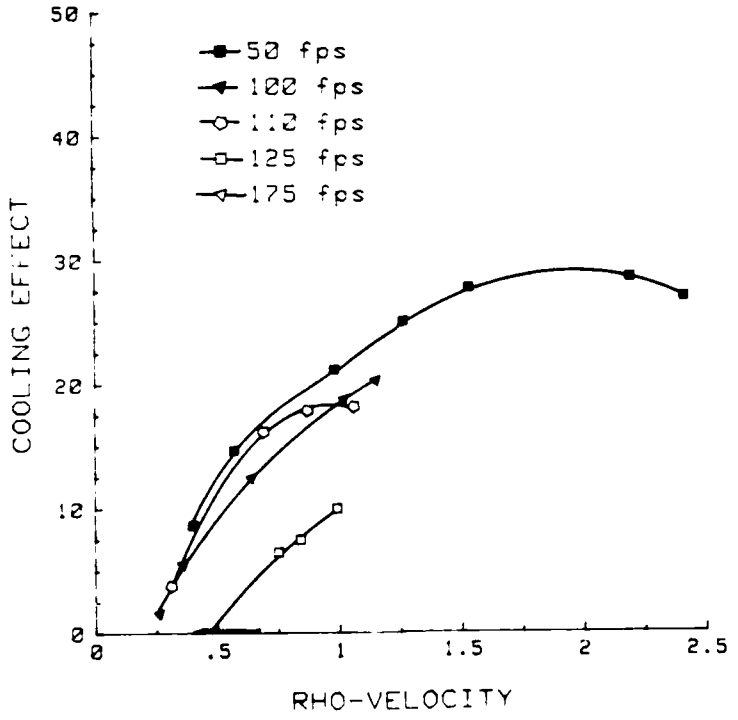

Figure 13 X/D = 22, Tu = 15.0 - 16.1%

Figure 14 displays little or no cooling effectiveness, thus the coolant is mixed to the point where the effects of film cooling are nearly gone.

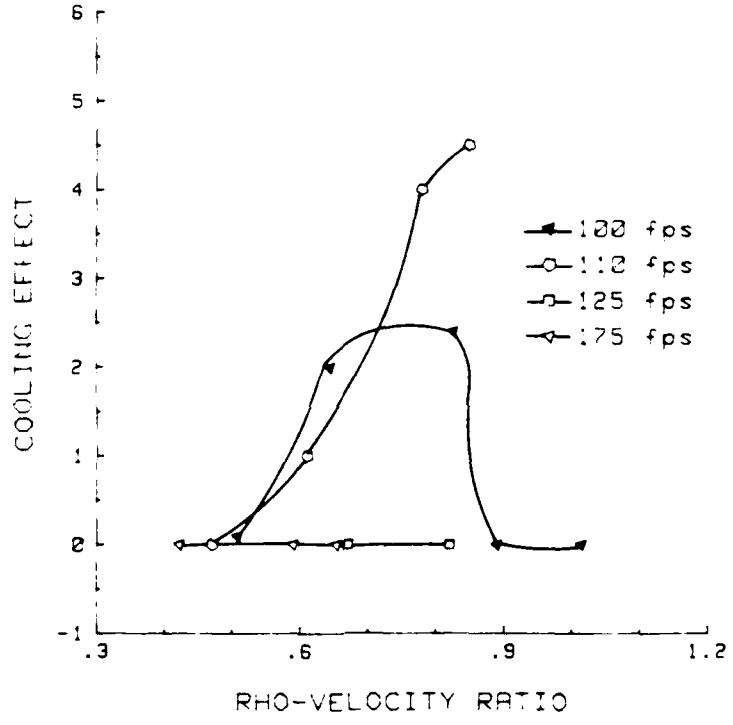

Figure 14 X/D = 42, Tu = 15.5 - 18.5%

Another way to view the effects of turbulence intensity on cooling effectiveness is to display fixed free-stream velocities (fixed Reynolds number) at specific stations down the plate. As the Reynolds number increases down the plate, film cooling effectiveness decreases. Keeping in mind, the effects on cooling effectiveness are effects that occur in the boundary layer. For a given free-stream turbulence, boundary layer turbulence increases with Reynolds number. Increasing free-stream turbulence, increases boundary layer turbulence for the same Reynolds number. The Reynolds number increased either by increasing the free-stream velocity or by increasing the distance down the plate. Reynold numbers varied from 1.16 - 5.45 X 10^6 and turbulence intensity varied from 14.3 - 17.0%. These results for 50 - 125 fps are displayed on Figures 15, 16, 17, and 18.

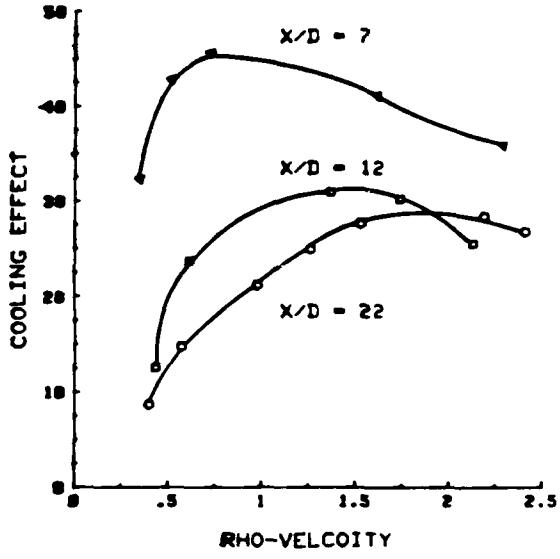

Figure 15 50 fps, Tu = 14.3 - 15.0%

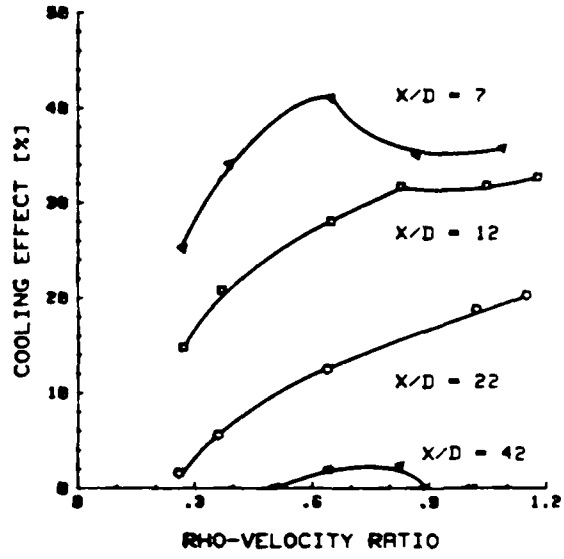

Figure 16 100 fps, Tu = 14.0 - 15.5%

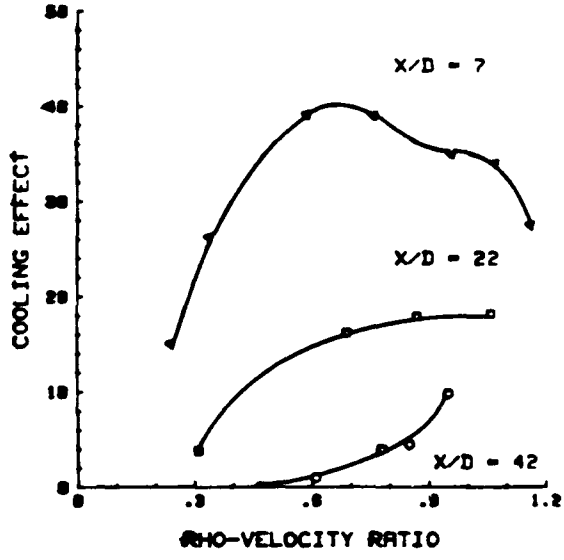

Figure 17 110 fps, Tu = 13.5 - 17.0%

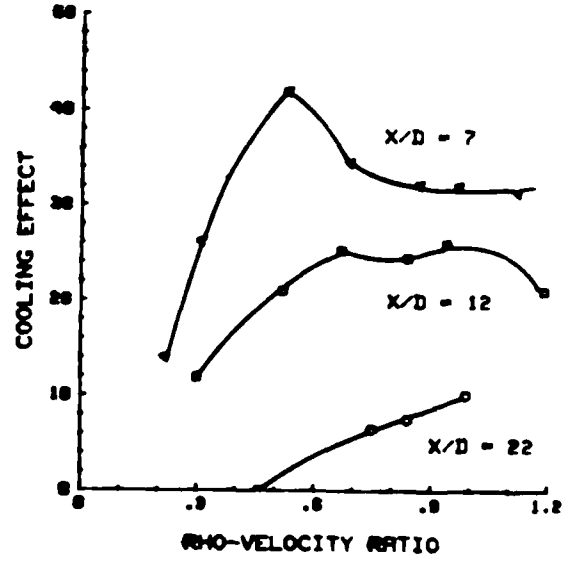

Figure 18 125 fps, Tu = 13.6 - 17.0%

Figures 15 - 18 show the decrease in film cooling effectiveness, but the results are stronger at the higher velocities as shown in Figure 19:

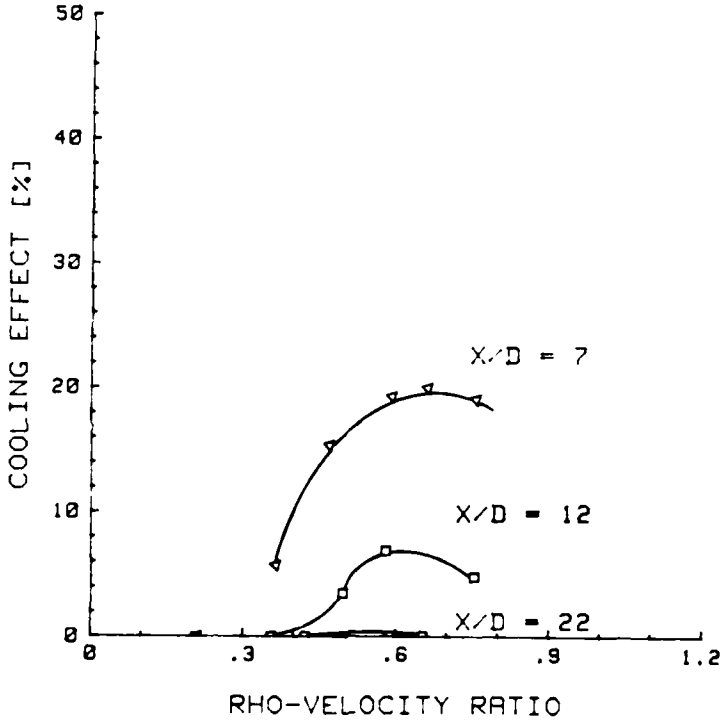

Figure 19 175 fps, Tu = 15.5 - 18.5%

Cooling Effectiveness vs. Distance down the plate:

The second major relationship is cooling effectiveness vs. distance down the flat plate. At each station, the free-stream velocity was fixed so the Reynolds number varied only by position down the plate. Blowing rates above and below optimum were tested. Turbulence intensities varied from 13.5 - 18.5%. The results of this parameter relationship displayed an almost exponential decay type of behavior. The general pattern is displayed in Figure 20 for a range of station velocities.

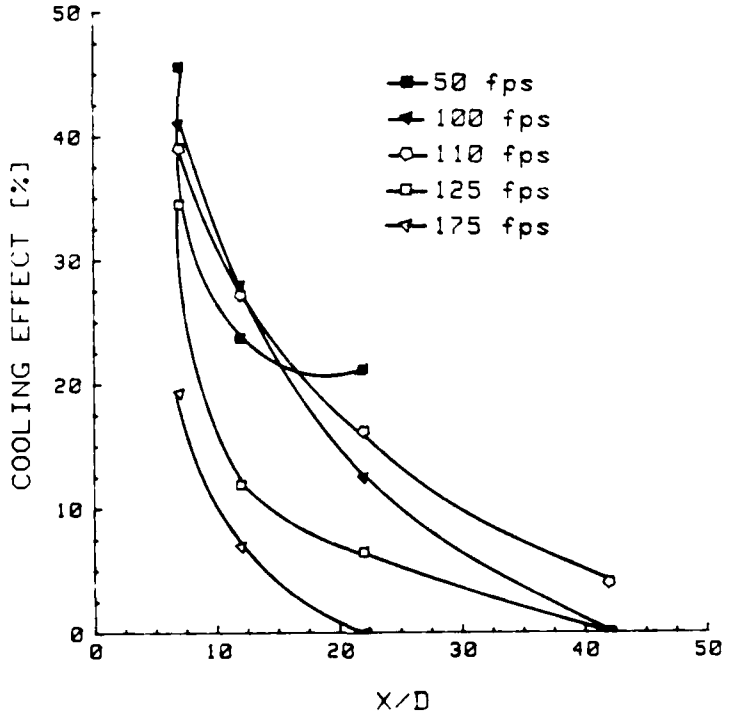

Figure 20 $M = 0.6$, $U_\infty = 50 - 175$ fps
$Tu = 13.5 - 18.5\%$

The rate of decay in cooling effectiveness appears to be related to the Reynolds number. For lower Reynolds numbers, the decay is not as rapid when compared to higher Reynolds numbers. Also, the distance down the plate at which cooling effectiveness can be measured is also related to the Reynolds number. For lower velocities, 50 fps, cooling effectiveness is relatively high when compare to higher velocities, 175 fps. Figures 21, 22, 23, and 24 display the effects of varing the blowing rate parameter, above and below optimum, on cooling effectiveness down the plate. Each curve tends to display the same decaying behavior.

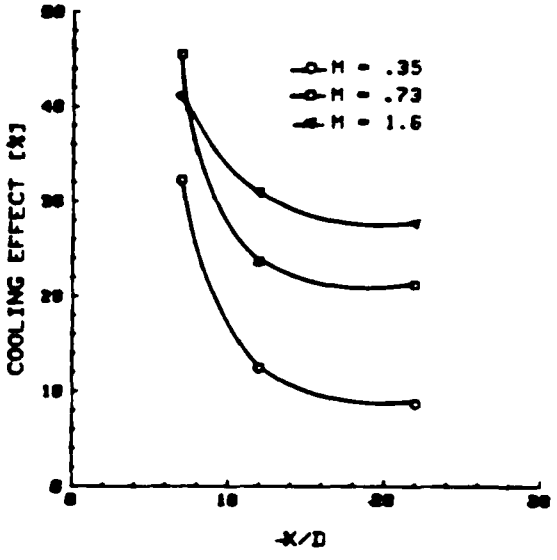

Figure 21 50 fps, Tu = 14.3 - 15.0%

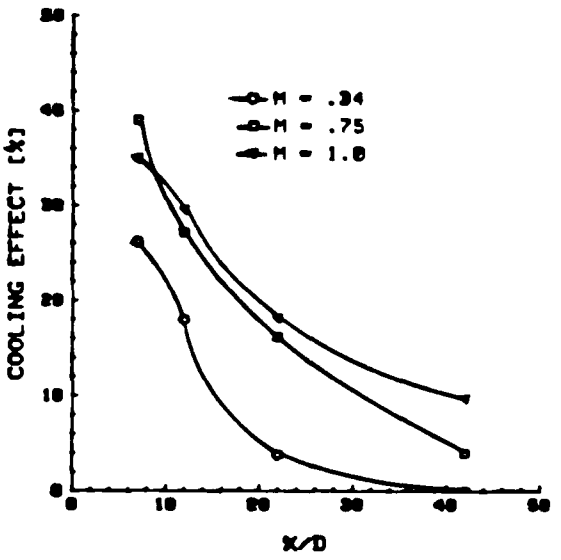

Figure 22 110 fps, Tu = 13.5 - 17.0%

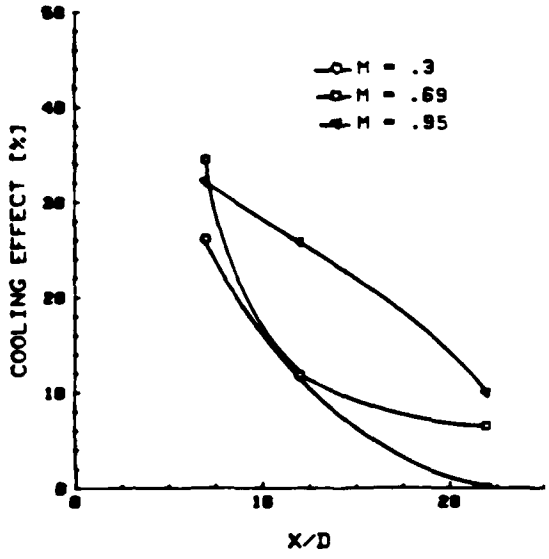

Figure 23 125 fps, Tu = 13.6 - 17.0%

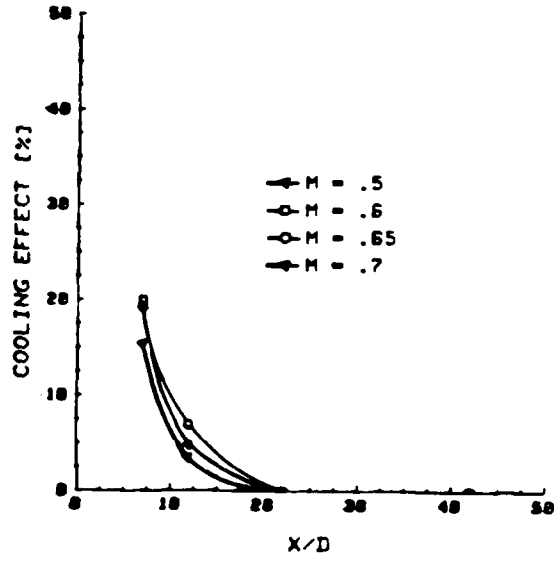

Figure 24 175 fps, Tu = 15.5 - 18.5%

Higher Reynolds numbers or higher free-stream turbulence produce higher levels of boundary layer turbulence intensities. The effect on film cooling effectiveness appears to be very much like an exponential decay. In chapter IV, a film cooling model was developed which relates film cooling effectiveness to Reynolds number. The film cooling model predicted that for higher Reynolds numbers, film cooling effectiveness would tend to decay faster with an exponential behavior. Figures 20 - 24

display an exponential decay type of behavior similiar to the cooling effect model developed in Chapter IV:

$$\frac{\eta}{\eta_o} = \frac{T - T_\infty}{T(0) - T_\infty} = e^{-C^* Re^{0.7} \left(1 - \left(\frac{H_o}{H'}\right)\right)^{0.7}}$$

If at least two points are known on the curve and if perfect mixing occured, the turbulence model could be used to predicted film cooling effectiveness at the point of injection and to determine the constant in the exponent. Using the turbulence model for 50, 110, and 175 fps resulted an ideal film cooling effectiveness at the point of injection of approximately 41%. More importantly, the model results displayed the relationship of Reynolds number to film cooling effectiveness. Increasing the Reynolds number (increasing turbulence intensity), increases the decay rate in cooling effectiveness. Figure 25 shows the model results for 50, 110, and 175 fps.

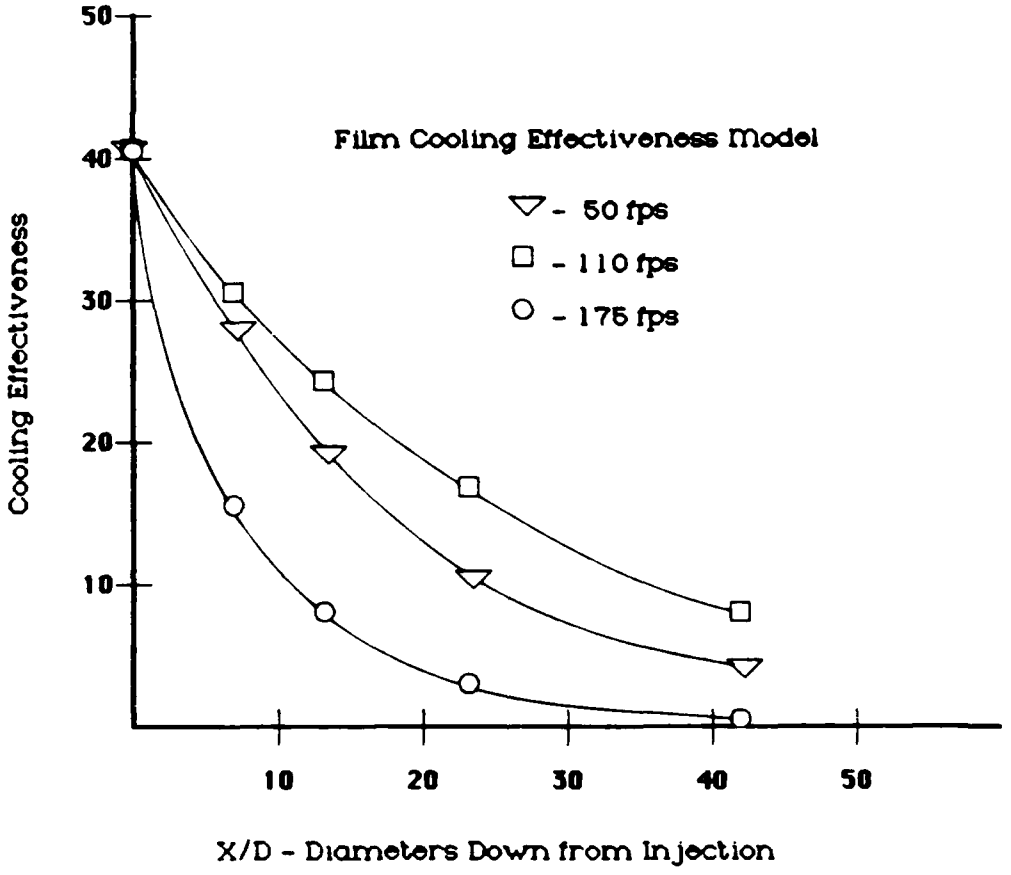

Figure 25 Film Cooling Model Plot

Figure 26 compares the film cooling model results with experimentally measured data for 110 and 175 fps. The turbulence model resulted in film cooling effectiveness values within 10% of experimentally measured data and displayed the dependence on Reynolds number.

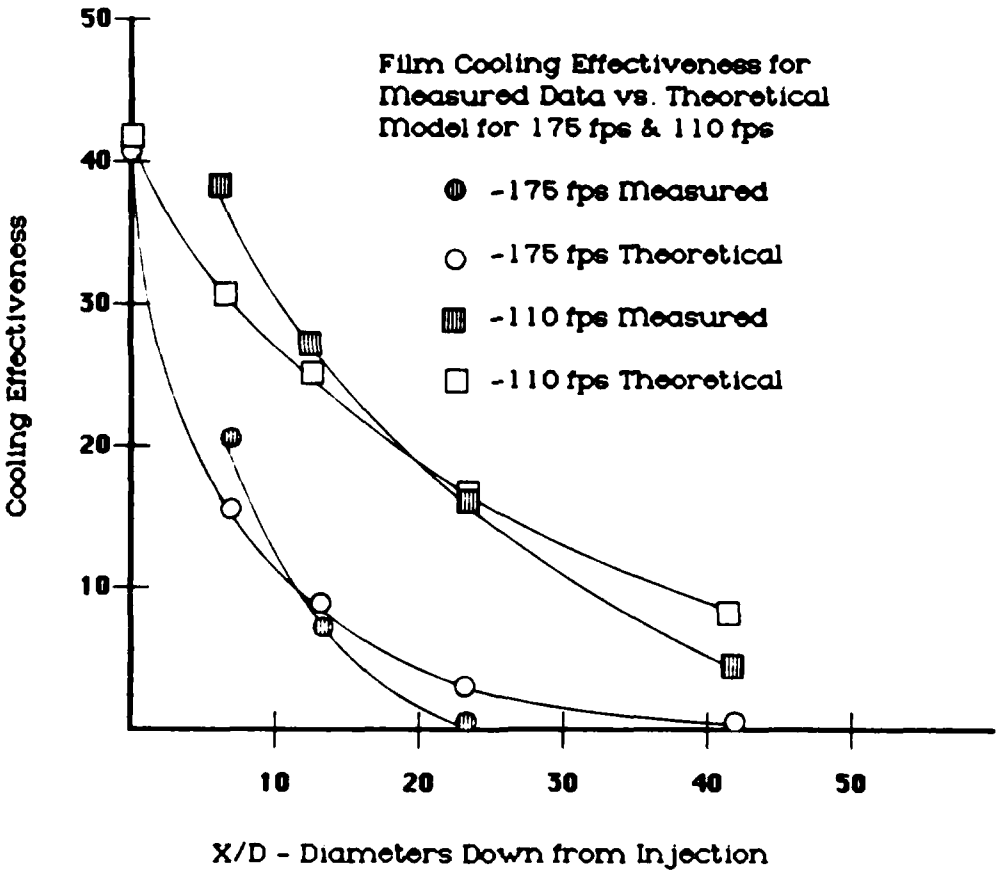

Figure 26 Model vs. Experimental Plot

Other work on film cooling effectiveness, such as J. C. Han, was done in wind tunnels at low levels of free-stream turbulence intensity. Han's work, at Re = 2×10^4 and turbulence intensities of approximately 5%, for 160 fps found about 14.5% cooling effectiveness at 40 diameters down-stream of injection, where in the present study, no film cooling effectiveness was found past 22 diameters. The reason for the faster decay is the higher free-stream turbulence. Figure 27 shows Han's results compared to the present study.

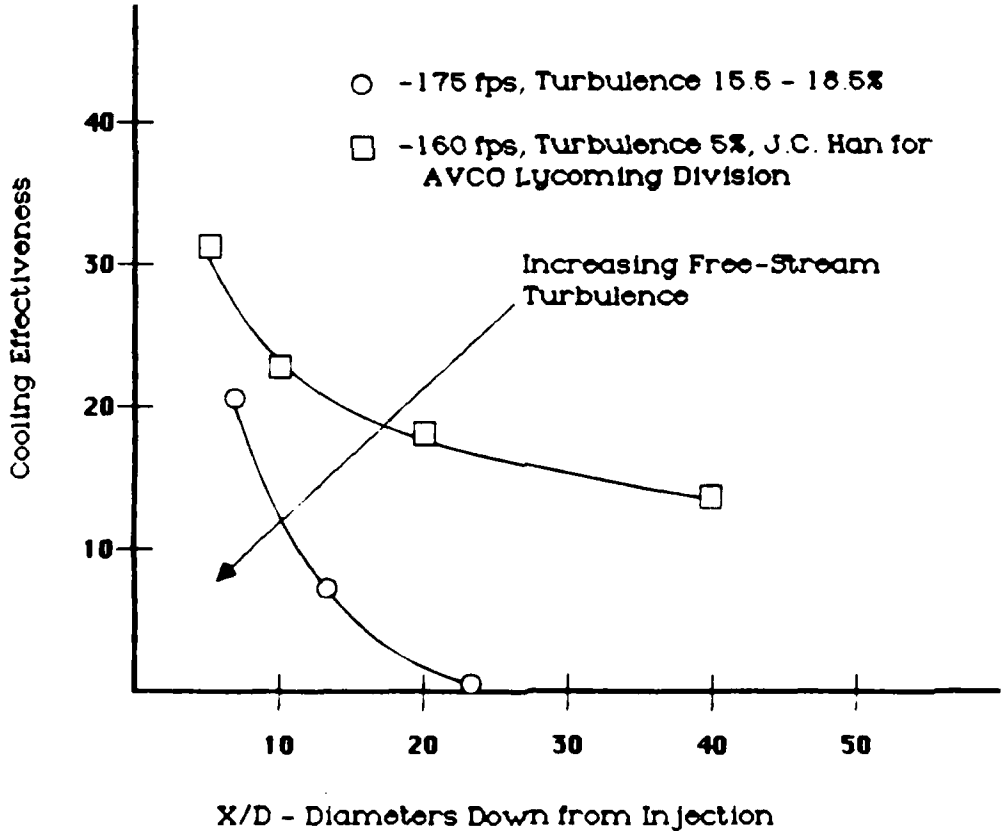

Figure 27 Comparison Plot

Cooling Effectiveness vs. Velocity:

The third relationship is cooling effectiveness vs. velocity for a fixed blowing rate and station on the plate. The idea was to see, for a blowing rate around optimum, if there is a Reynolds number based on velocity which produces an optimum cooling effectiveness. The results proved very surprising. At X/D = 42, Figure 28, when cooling effectiveness could be measured, cooling effectiveness peaked at a Reynolds number around 5.45×10^6 for a free-stream velocity 110 fps. At X/D=22, Figure 29, the effect became more pronounced at a Reynolds number of 4.36×10^6, for a free-stream velocity of 110 fps. The "best" behaved results occured at X/D = 12, Figure 30, where all the curves peaked at a Reynolds number of 3.80×10^6, again a free-stream velocity of 110 fps. At X/D = 7, Figure 31, all the curves remained around 40% cooling effectiveness until a Reynolds number of 3.58×10^6, again a free-stream velocity of 110 fps, and then cooling effectiveness rapidly decreased. Turbulence intensity at 110 fps was an average for all the tests varing from 13.5 - 18.5%. The reason for the jumps in the data at 110 fps is unclear, but Figures 28 - 31 all show a rapid decrease in cooling effectiveness at higher free-stream velocities. Some phenomenon

is occuring in the flow around 110 fps which is not understood. Data on integral length scale and power density spectra need to be obtained.

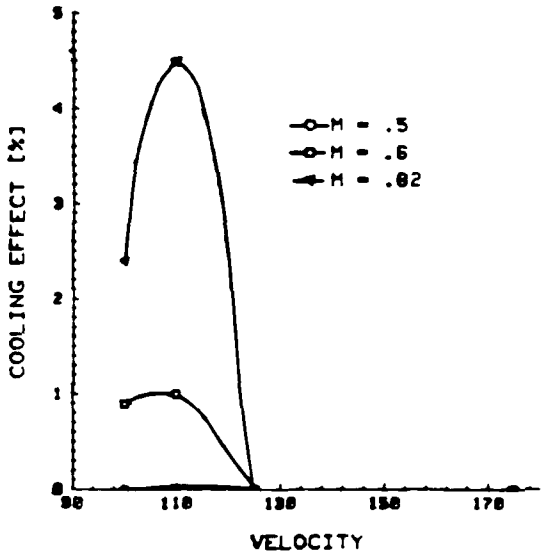

Figure 28 X/D = 42, Tu = 15.5 - 18.5%

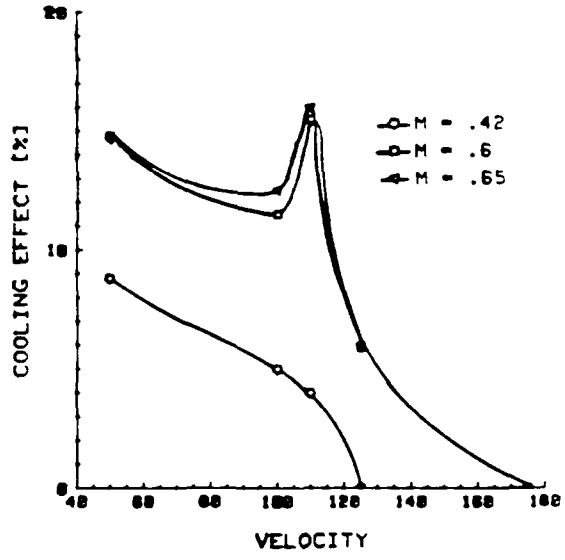

Figure 29 X/D = 22, Tu = 15.0 - 16.1%

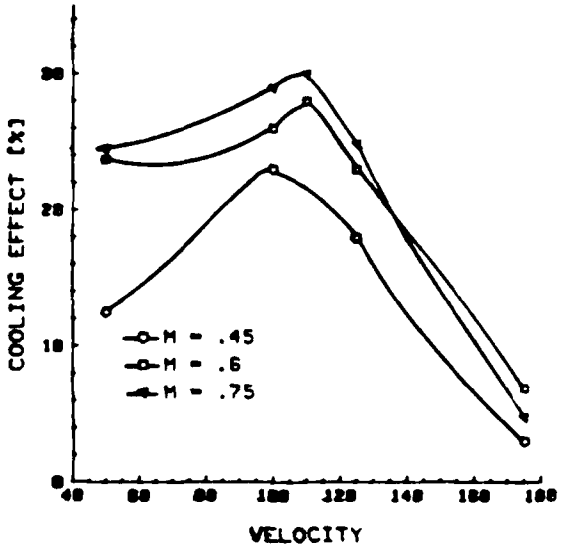

Figure 30 X/D = 12, Tu = 15.0 - 15.8%

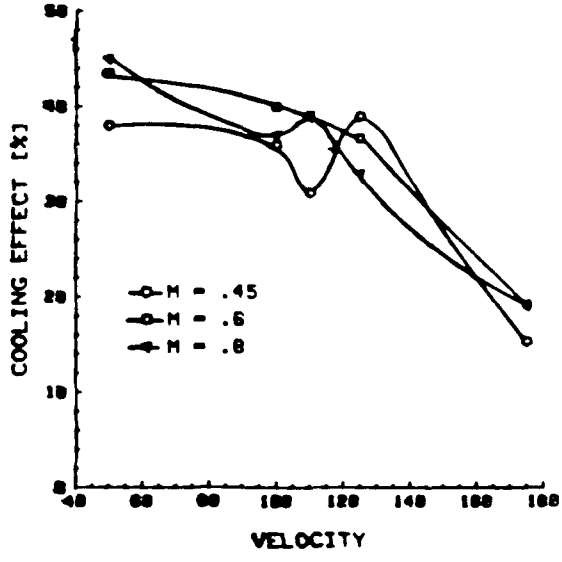

Figure 31 X/D = 7, Tu 14.3 - 15.5%

The significance of this study is more apparent when compared with other work done in this area, specifically the references in chapter I. The turbulence intensity of the present study was 13.5 - 18.5% compared to 5% in work done by Goldstein and Han. Two major conclusions can be made about film cooling effectiveness in high free-stream turbulence. First, optimum cooling effectiveness occurs at approximately the same blowing rate range regardless of turbulence intensity levels or Reynolds number. Second, film cooling effectiveness down the plate decreased more rapidly at higher turbulence intensities.

Optimum Cooling Effectiveness vs Blowing Rate:

Both Goldstein's work at low free-stream velocities around 50 fps and Han's work at high free-stream velocities around 168 fps show the optimum cooling effectiveness occured for a blowing rate parameter in the range of 0.5 - 0.6 for slant hole injection and within 10 diameters down-stream of injection. The results of the present study were the same.

Film Cooling Effectiveness Down the Plate:

Both Goldstein and Han found results around 10% film cooling effectiveness at 40 diameters down-stream of injection. In the present study, little to no film cooling effectiveness was found at 40 diameters. In fact, at the highest Reynolds numbers and turbulence intensities tested, there was no film cooling effectiveness past 22 diameters down-stream of injection. The turbulence model, developed in Chapter IV, predicted a faster decay in cooling effectiveness at higher Reynolds numbers. Experimentally measured data followed this trend, thus higher free-stream turbulence intensities result in fast decay of film cooling effectiveness.

Velocity/Temperature Profiles

The purpose of this test was to obtain a velocity/temperature profile and to ensure the boundary layer did not seperate for a blowing rate parameter of 0.6. Although boundary layer seperation was checked before all tests, a plot of the profiles displays not only had seperation not happened, but also the profiles were typical of a turbulent boundary layer profiles. Station 3 was selected to be sure the data was collected

well down-stream of the mixing region. The results are plotted on Figures 32 and 33 indicate seperation did not occur and the effects of the mixing region, displayed in Figure 8, where not present.

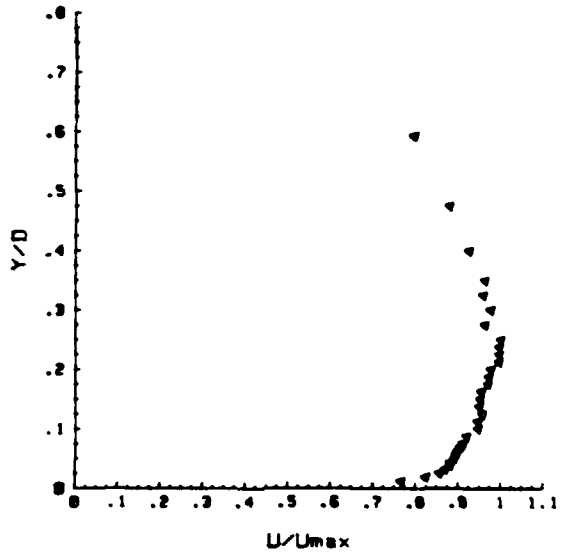

Figure 32 Velocity Profile, 175 fps
Tu = 16.1%, M = 0.6

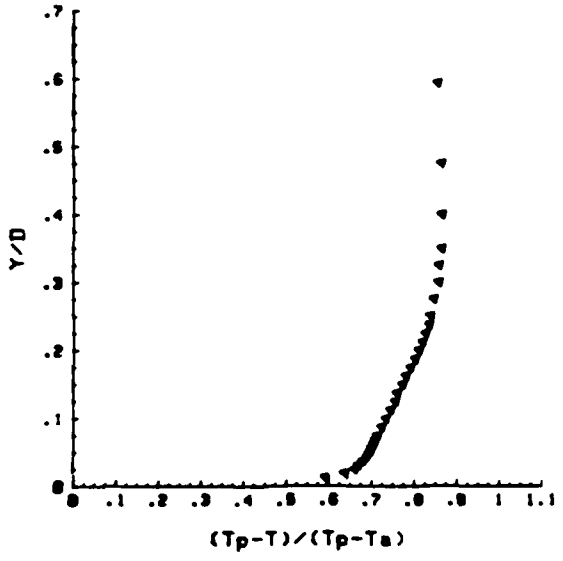

Figure 33 Temperature Profile,
175 fps, Tu = 16.1%, M = 0.6

Heat Transfer

The heat transfer test were done for a blowing rate parameter of 0.6 and station velocities of 175 fps which resulted in turbulence intensity range of 15.5% at station 1 to 18.5% at station 4. The data is presented as Stanton and Nusselt numbers with blowing divided by Stanton and Nusselt number wihtout blowing. The results displayed in Figure 34 indicated two interesting points. First the Stanton and Nusselt plots were nearly identical. Second, past 22 diameters down-stream of injection, the ratios were greater than one. Logically thinking, at best, the ratio would aproach 1.0, but not greater. Other work done by Goldstein indicates that down-stream the ratio are near one. Sometimes slightly greater or slightly less than 1.0, perhaps values greater than 1.0 were due to measurement errors. Comparison with Goldstein's work is not really possible because his primary and secondary flows were at the same temperature. In the present study, there was about a 10° F difference in the two flows. The original idea was to provide a temperature gradient from the plate to the free-stream. The plate was the hottest, about 100° F, the secondary flow next, about 90° F, and the coolest was the free-stream at about 80° F. Although the temperature

difference between the main and secondary flows is small, it still has an effect on heat transfer. The thinking was to simulate a turbine blade using film cooling, other than porous injection, where the primary and secondary flows would be at different temperatures. The preliminary results of this study indicate that perhaps for different temperature flows, the local ratio of Stanton number with blowing to without might be greater than 1.0. Since there is no similar work, it is not possible to make comparisons. Further heat transfer tests are recommended.

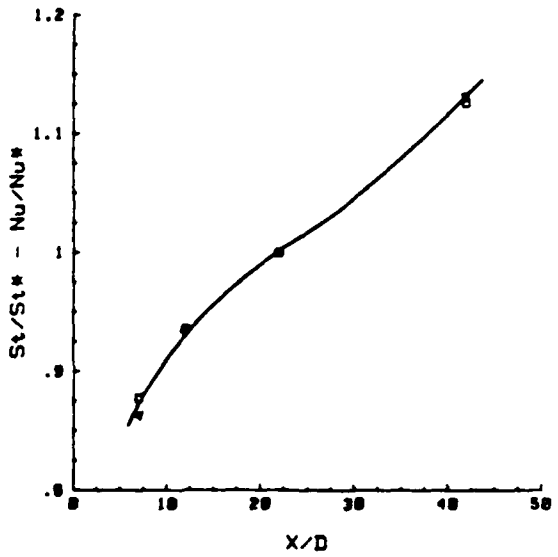

Figure 34 St/St* - Nu/Nu*, 175 fps,
Tu = 15.5 - 18.5%

VI. Conclusion

1. Turbulence intensity has little effect on the blowing rate for optimum film cooling effectiveness within 10 diameters down-stream of injection.

2. Turbulence intensity has a strong effect on decreasing film cooling effectiveness down-stream of the injection.

3. Some phenomenon is occurring in the flow at 110 fps which is not understood in this study.

VII. Recommendations

1. Before any further tests are conducted, the air supply system must be modified to eliminate oil contamination of the flow.

2. A "wind tunnel" type cover over the plate is recommended to try to control turbulence scale and turbulence intensity independently. The cover will also help to reduce environmental effects of the control room on the flat plate. This should also help when comparing data to tests done in a wind tunnels.

3. With the covered table, heat transfer data should be taken using the same methods used by Goldstein.

4. Flow visualization is recommended along with three-dimensional laser techniques to measure flow properties.

5. The circular nozzle should be replaced with a narrow rectangular slot to increase the range of X/D.

6. The traversing system should be rebuilt to reduce vibration. Vibration damaged the probes during measurements at less than .01 inches from the table.

Bibliography

1. Goldstein, R. J. and others. Flow And Temperature Fields Following Injection of a Jet Normal to a Cross Stream. FC(b)-14, pp. 255-260.

2. Goldstein R. J. and others. "Film Cooling With Injection Through Holes: Adiabatic Wall Temperatures Downstream of a Circular Hole," Journal of Engineering for Power, pp 384-395 (Oct 1968).

3. Goldstein R. J. and others. "Effects Of Hole Geometry And Density On Three-Dimensional Film Cooling," International Journal Heat mass Transfer, vol. 17, pp. 595-607 (1974).

4. Han J. C. and Mehendale, A. B. Flat-Plate Film Cooling With Steam Injection Through One Row and Two Rows of Inclined Holes, ASME, Paper 86-GT-105.

5. Han, J. C. and Mehendale, A. B. Film Cooling and Heat Transfer With Steam Injection Through Inclined Circular Holes, AVCO Lycoming Division. Contract N-832132-E, May 1985.

6. Bejan, Adrian. Convection Heat Transfer. New York: John Wiley & Sons, 1984.

7. MacArthur, C. D. Fluid Dynamics and Heat Transfer of the Circular Tangential Wall Jet. Ph.D. Dissertation, University of Dayton, Dayton, OH, April 1986.

8. Schlichting, H. Boundry Layer Theory (7th Edition). New York: McGraw-Hill Book Company.

9. Kays, W. M. and M. E. Crawford. Convective Heat and Mass Transfer (Second Edition). New York: McGraw-Hill Book Company, 1980.

10. Goldstein, R. J. "Film Cooling," Advances in Heat Transfer, vol. 7, pp.321-379 (1979).

11. Goldstein, R. J. and Eriksen, V. L. "Heat Transfer and Film Cooling Following Injection Through Inclined Circular Tubes," Journal of Heat Transfer, pp.239-245 (May 1974).

12. Goldstein, R. J. and others. NASA CR-54606, 1968.

13. Holman, J. P. Heat Transfer (4th Edition). New York: Mcgraw-Hill Book Company.

14. Shapiro, A. H. The Dynamics and Thermodynamics of Compressible Flow (Volume 1). New York: John Wiley & Sons, 1953.

15. Han, J. "Effect of High Free-Stream Turbulence from a Free Jet on Flat Plate Turbulent Boundry Layer Flow and Heat Transfer," 1985 USAF-UES Summer Faculty Research Program, Contract F49620-85-C-0013, 30 August 1985.

16. MacMullin, Major Robert. Effects of Free - Stream Turbulence From A Circular Wall Jet On Flat Plate Heat Transfer And Bountry Layer Eolw. MS thesis, AFIT/GA/AA/86D-10. School of Engineeting, Air Force Institute of Technolgy (AU), Wright-Patterson AFB, OH, December 1986.

17. Hinze, J. O. Turbulence. New York: McGraw-Hill Book Company, 1959.

18. Crawford, H. and others. Full - Coverage Film Cooling on Flat, Isothermal Surfaces: A Summary Report on Data and Predictions. NASA Contractor Report 3219, January 1980.

19. Webster W. P. and Yavuzkurt S. Measurements of Mass Transfer Coefficient and Effectiveness in the Recovery Region of A Film-Cooled Surface. ASME, Paper No. 86-GT-134.

20. Fluid Meters, Their Theory and Applications(Sixth Edition). ASME (1971).

VITA

Geoffrey W. Jumper was born on 8 March 1952 in Albuquerque, New Mexico. He graduated from Del Oro High School, Loomis, California, attended two years at the University of New Mexico, then attended and graduated from the U.S. Air Force Academy in 1976 with a degree of Bachelor of Science in Civil Engineering. He recieved his commision in the U.S. Air Force in 1976 and completed Undergraduate Pilot Training (UPT) at Williams AFB, Arizona. Upon graduation from UPT, he was assigned to 62 Tactical Airlift Squadron (TAS), Little Rock AFB, Arkansas to fly the C-130. In 1979, he was assigned to the 37 TAS, Rhein Main AB, West Germany and in 1982 reassigned to 62 TAS in Little Rock AFB. During that time, he served in all areas of tactical airlift to include flight examiner pilot. In 1982 he completed Squadron Officers School in residence, and in 1984 he completed Air Command and Staff College by seminar. While at Little Rock AFB, he graduated from the University of Arkansas with a Masters of Science degree in Operations Management.

REPORT DOCUMENTATION PAGE

Form Approved
OMB No. 0704-0188

1a. REPORT SECURITY CLASSIFICATION
UNCLASSIFIED

1b. RESTRICTIVE MARKINGS
AD-A190 500

2a. SECURITY CLASSIFICATION AUTHORITY

2b. DECLASSIFICATION / DOWNGRADING SCHEDULE

3. DISTRIBUTION / AVAILABILITY OF REPORT
Approved for public release; distribution unlimited.

4. PERFORMING ORGANIZATION REPORT NUMBER(S)
AFIT/GAE/AA/87D-7

5. MONITORING ORGANIZATION REPORT NUMBER(S)

6a. NAME OF PERFORMING ORGANIZATION
School of Engineering, Air Force Institute of Tech.

6b. OFFICE SYMBOL (If applicable)
AFIT/ENY

7a. NAME OF MONITORING ORGANIZATION

6c. ADDRESS (City, State, and ZIP Code)
Wright-Patterson AFB, Ohio 45433-6563

7b. ADDRESS (City, State, and ZIP Code)

8a. NAME OF FUNDING / SPONSORING ORGANIZATION
Aero Propulsion Laboratory

8b. OFFICE SYMBOL (If applicable)
AFWAL/POTC

9. PROCUREMENT INSTRUMENT IDENTIFICATION NUMBER

8c. ADDRESS (City, State, and ZIP Code)
Wright-Patterson AFB, Ohio 45433-6563

10. SOURCE OF FUNDING NUMBERS

PROGRAM ELEMENT NO.	PROJECT NO.	TASK NO	WORK UNIT ACCESSION NO.

11. TITLE (Include Security Classification)
Film Cooling Effectiveness on a Flat Plate in High Free-Stream Turbulence Using a Single Row of 30° Slant-Hole Injectors (Unclassified)

12. PERSONAL AUTHOR(S)
Geoffrey W. Jumper, Major, U.S. Air Force

13a. TYPE OF REPORT	13b. TIME COVERED	14. DATE OF REPORT (Year, Month, Day)	15. PAGE COUNT
MS THESIS	FROM _____ TO _____	1987, December, 2	79

16. SUPPLEMENTARY NOTATION

Approved for public release: IAW AFR 190-1.
LYNN E. WOLAVER 31 Dec 87
Dean for Research and Professional Development
Air Force Institute of Technology (AU)
Wright-Patterson AFB OH 45433

17. COSATI CODES		
FIELD	GROUP	SUB-GROUP
20	13	
20	04	

18. SUBJECT TERMS (Continue on reverse if necessary and identify by block number)
Free-Stream Turbulence Boundary Layer Flow
Flat Plate Film Cooling Effectiveness
Wall Jet

19. ABSTRACT (Continue on reverse if necessary and identify by block number)

In the continuing search to understand the mechanisms influencing film cooling effectiveness, this thesis examines film cooling effectiveness on a flat plate in high free-stream turbulence using a single row of 30° slant-hole injectors. The primary area of focus is the area within 42 diameters downstream of injection, and the decay of film cooling effectiveness down the plate. Free-stream velocities from 50-175 feet per second and free-stream turbulence intensities from 13.5-18.5% were examined. Changes in Reynolds number or free-stream turbulence had little effect on blowing rates for optimum film cooling effectiveness. In comparison with tests conducted in low free-stream turbulence, around 5%, higher free-stream turbulence causes a faster decay in film cooling effectiveness down the plate.

20. DISTRIBUTION / AVAILABILITY OF ABSTRACT
☒ UNCLASSIFIED/UNLIMITED ☐ SAME AS RPT ☐ DTIC USERS

21. ABSTRACT SECURITY CLASSIFICATION
Unclassified

22a. NAME OF RESPONSIBLE INDIVIDUAL
Dr. William C. Elrod

22b. TELEPHONE (Include Area Code)
513-255-3517

22c. OFFICE SYMBOL
AFIT/ENY

DD Form 1473, JUN 86 *Previous editions are obsolete.*

END

DATE

FILMED

4-88

DTIC